



Article

Coniferous Trees as Bioinspiration for Designing Long Reinforced Prestressed Concrete Columns

Traian-Nicu Toader ^{1,*}, Călin G.-R. Mircea ¹, Alina M. Truta ² and Horia Constantinescu ¹

¹ Department of Structures, Faculty of Civil Engineering, Technical University of Cluj-Napoca, Str. Constantin Daicoviciu 15, 400020 Cluj-Napoca, Romania; calin.mircea@dst.utcluj.ro (C.G.-R.M.); horia.constantinescu@dst.utcluj.ro (H.C.)

² Department of Forestry, University of Agricultural Sciences and Veterinary Medicine, Str. Calea Mănăştur 3–5, 400372 Cluj-Napoca, Romania; alina.truta@usamvcluj.ro

* Correspondence: traian.toader@dst.utcluj.ro

Abstract: This article contains the results of identifying the potential of coniferous trees to act as bioinspiration for the structural design of columns in single-story warehouses subjected to high wind velocity and severe seismic action. This study starts by analyzing the biomechanics of coniferous trees, continues with an abstraction of the relevant features, and ends with the transfer of a design methodology for long reinforced and prestressed concrete columns. To verify the applicability and validity of the mathematical relationships extracted from the bibliographic study to characterize the biomechanics of coniferous trees, a study site is conducted for Norway spruce trees felled by the wind in the Bilbor area. The design methodology for long reinforced and prestressed concrete columns bioinspired by the Norway spruce trees is experimentally validated using two case studies. The first case study deals with the effect of centric prestressing on long concrete columns, and the second on the influence of the walnut shell powder on the adhesion of the reinforcement in concrete. The case studies presented aim to transfer some characteristics from trees to reinforced concrete to improve the performance of long columns under horizontal forces. The results obtained indicate a good approximation of the trees' structural behavior for this site and for ones investigated by other researchers in different forests.

Keywords: biomimetic concrete column; Norway spruce; prestressed reinforced concrete; biomechanics; energy dissipation; walnut shell



Citation: Toader, T.-N.; Mircea, C.G.-R.; Truta, A.M.; Constantinescu, H. Coniferous Trees as Bioinspiration for Designing Long Reinforced Prestressed Concrete Columns.

Biomimetics **2024**, *9*, 165. <https://doi.org/10.3390/biomimetics9030165>

Academic Editors: Shupeng Wang, Pengyun Xu and Yangyang Wei

Received: 2 February 2024

Revised: 27 February 2024

Accepted: 5 March 2024

Published: 7 March 2024



Copyright: © 2024 by the authors. Licensee MDPI, Basel, Switzerland. This article is an open access article distributed under the terms and conditions of the Creative Commons Attribution (CC BY) license (<https://creativecommons.org/licenses/by/4.0/>).

1. Introduction

People's needs for sheltering new technological processes in factories, storing material goods in modern logistics centers, and building mega shopping centers have been materialized through projects of single-story constructions with significant heights on sites with severe seismic actions [1]. The need for large free heights of 10 m and above results from the organization of technological flows and the good functionality of the building, while the site is chosen mainly according to the development of the infrastructure and the workforce available for future economic activity [2]. Considering the above criteria, it is observed that the free height of the columns that make up these structures is almost impossible to reduce, thus the structural engineer is responsible for finding solutions suitable for the design theme, which must also be economically competitive and in line with sustainable development.

In nature, materials have specifications starting from the atom level, such as spider silk, wood, shells, etc. People have imitated nature by creating new synthetic materials such as cement materials (e.g., concrete) [3,4] and alloys (e.g., steel), sometimes starting at the atom level, such as Nylon and Kevlar [5].

Columns are crucial structural elements in a load-bearing structure. They have the role of transferring the loads applied at roof level, on the facades, and those on their height

to the foundations. In single-story warehouses (Figure 1), the columns are often subjected to high eccentric compression and shear force, identical to trees. From a mechanical point of view, the trunks of trees have the role of transferring the loads applied to the crown and trunk (own weight of the branches and trunk, precipitations, and wind action) to the root system [6–9]. For both columns and trees, the static scheme is that of a vertical cantilever embedded at the base. As the length of the cantilever increases, it is necessary to increase the bending stiffness to avoid excessively large lateral displacements leading to loss of stability; therefore, it is necessary to increase the resisting bending moment to be able to take up the demanding bending moment, otherwise the cantilever would break in the most severely stressed cross-section. The bending stiffness can be expressed as $E \cdot I$, where E is a mechanical characteristic of the material (longitudinal modulus of elasticity) and I is a geometric characteristic of the section (moment of inertia or, more specifically, second moment of area). Therefore, to obtain a higher bending stiffness, we need to increase at least one of the terms. If we keep the materials used, it follows that increasing the stiffness can only be achieved by increasing the dimensions of the cross-section.



Figure 1. Load-bearing structure for a single-story warehouse on a site with severe seismic action, ground acceleration $a_g = 0.35$ g. Reproduced with permission from ©SDC Project [https://www.sdcproject.ro/wp-content/uploads/2018/10/IMG_1887-08-06-18-11-30-1.jpg (accessed on 4 March 2024)].

Nowadays, the most used and financially accessible building materials are concrete and steel. Concrete has physical (high resistance to fire and aggressive environment, medium specific weight, low thermal expansion, etc.) and mechanical properties (sufficient compressive strength, favorable elasticity mode, etc.) that make it recommendable for widespread use in load-bearing structures. However, the low tensile strength of concrete is an impediment, involving its association with other reinforcement materials (with tensile strength 100 to 1000 times that of concrete), resulting in a composite material, i.e., reinforced concrete [10]. An excellent reinforcement in concrete is steel in the form of ribbed bars. Steel has a thermal expansion compatible with that of concrete and good adhesion when embedded. When reinforced concrete structures exhibit deformations above the serviceability limits, or when the goal is to reduce the dimensions and the elements' own weight, active reinforcement (pre-tensioned or post-tensioned) can be used in association with the concrete, thus resulting in a composite material like the first but with superior mechanical performance, i.e., prestressed concrete. In the modern era, engineering solutions for the reinforcement (using passive reinforcement) of reinforced concrete have been studied and then successfully implemented by engineers and professors such as Emil Mörsch and Fritz Leonhardt [11–16]. Regarding prestressed concrete, prestressing engineering solutions were studied and successfully applied in construction by the pioneering French builder

Freyssinet and immediately continued by his successors [17–19]. Since the beginning of the modern use of reinforced concrete, the strut-and-tie model and the stress-field model have been used as design principles, with reinforcements positioned inside the concrete member where tensile stresses would exceed the tensile strength of the concrete.

The purpose of this article is to identify the relevant mechanical, physical, dynamic, and morphological properties to verify the potential of coniferous trees (Figure 2) as a biological role model in the design of long reinforced and prestressed concrete columns. Being aware of existing differences, this article is focused on the similarities that can improve the design of this type of column and its foundations within single-story warehouses.

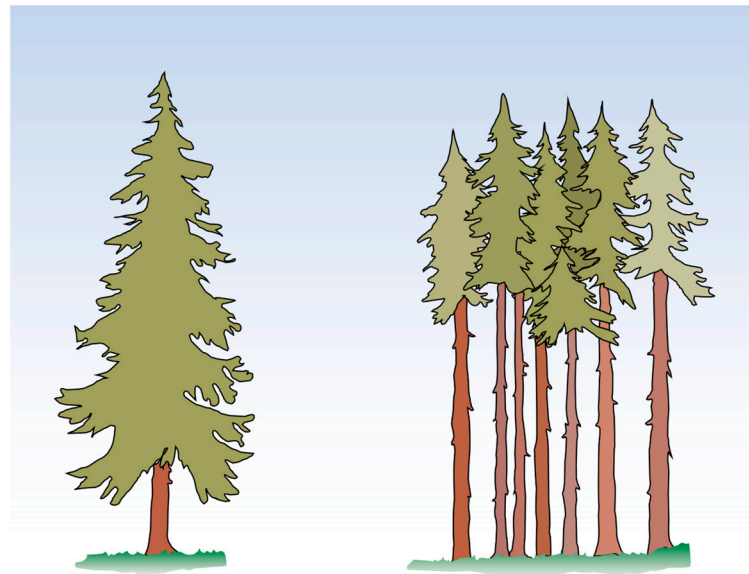


Figure 2. Coniferous forest trees (spruce species) as freestanding (left) versus densely growing (right). Adapted from ©Swedishwood [<https://www.swedishwood.com/optimized/default/siteassets/1-trafakta/2-att-valja-tra/01/com/fristaende-gran-com.jpg>] (accessed on 4 March 2024)].

In this article, bioinspiration is oriented towards a direct and pragmatic applicability in structural engineering, and, through biomimetics, an attempt is made to decipher the natural design strategy of coniferous forest trees transferring to long prestressed reinforced concrete columns and their foundations. The particularities of the trees are analyzed through the lens of biomechanics, considering as studied parameters statics, dynamics, morphology, rooting, and energy dissipation.

2. Analysis and Abstraction of the Biological Model

2.1. Biomimetics and Trees

Biology has a large potential to generate structural solutions for today's reinforced concrete constructions [20,21]. The present research aims to clarify how tall forest trees have an amazing ability to withstand high horizontal forces. The form–structure–model relationship is investigated by abstracting and adapting bioinspired load-bearing structures. Biological models are processed to understand the natural response and the natural balance within the structure. We must notice that such an approach does not explain the entire complexity of the natural biological role model but tries to discover the mechanical fundamentals through complex modeling of innovative reinforced and prestressed concrete members. Figure 3 shows the relationship between biology and technical implementation in case studies comprising analysis, abstraction, and implementation [22].

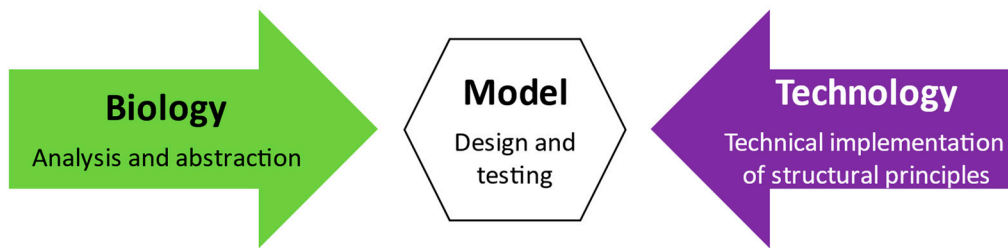


Figure 3. Interaction between the study of biology and technical implementation in biomimetics, based on [22].

2.2. Dynamics and Damping

Dynamics. Biomechanics studies trees as mechanical objects [23] using principles from engineering and physics to understand the structural properties of trees and how they interact with the environment. Tree growth rate is directly influenced by physiological aspects, especially those affecting photosynthesis and water transport [24]. But whether they are optimal or not, the size and shape of the tree is limited by biomechanical constraints [25]. Tree wood, as well as most plant materials, is viscoelastic because its mechanical properties are both elastic and viscous [26]. These properties involve a non-linear behavior [27,28], and, when mechanically stressed, live wood does not fit into a current mechanical model, as, for example, it does for concrete and steel. Thus, it is important to acknowledge the limitations of attempts to characterize and quantify trees using exact parameter values, and to recognize the failures when theory and reality do not coincide [29]. In addition, biological materials change their properties as trees grow and age [25,30–35], thus making the dynamic response difficult to predict.

Frequency. The frequency of swinging trees has been the subject of numerous studies and proposed relationships for the dominant frequencies of trunks [36–44]. Figure 4 shows a synthesis of the natural frequency determined on coniferous trees. Based on the cantilever beam model, Blevins [45] proposed the following relation for the natural vibration frequency:

$$f_n = \frac{\lambda^2}{2 \cdot \pi \cdot L^2} \cdot \sqrt{\frac{E \cdot I_0}{\rho \cdot A_0}} \quad (1)$$

where λ is a dimensionless parameter depending on the variations of the tree properties (e.g., shape, mass, and stiffness distribution), L is the height of the trunk, E is the elasticity modulus, I_0 is the second moment of area at the base (the basal area moment of inertia), ρ is the density of the material, and A_0 is the cross-sectional area at the base of the cantilever beam (trunk).

Furthermore, Scannell [46], Petty, and Swain [47] quantified the influence of the branches in decreasing the frequencies of the amplitude of the trunk swings. On the other hand, the empirical relationship proposed by Moore and Maguire [36] was validated for about 600 coniferous trees of different heights, diameters, and species:

$$f_n = 0.0948 + 3.4317 \cdot \frac{DBH}{L^2} - 0.7765 \cdot I_p \cdot \frac{DBH}{L^2} \quad (2)$$

where L is the height of the trunk, DBH is the diameter of the trunk measured at chest level (approximately 1.35 m above the ground), and I_p is a parameter equal to 1 if the genus is *Pinus* and 0 otherwise.

Damping. While the natural frequency of a tree is relatively easy to quantify and overall measure, the quantification of damping is much more complex [28]. Tree damping includes several components, e.g., (a) aerodynamic damping, (b) internal or viscoelastic damping, (c) mass damping, (d) damping by root–soil interaction, and (e) collision of branches or other crowns [28,48]. Figure 4 summarizes the frequency and damping values of about 900 coniferous trees of different sizes and masses, calculated and published

in [36–41,49–52]. However, the fraction of critical damping ξ (damping ratio) can vary greatly. In particular cases, it was observed that, due to the very high damping by the oscillations of branches (c) and the collision between branches (e), the trees were almost critically damped ($\xi \approx 100\%$), returning to their original position (rest position) after only one or two cycles of free vibration [49].

In the experimental and numerical studies of [49,53], it was observed that by removing the branches, the natural frequency of the tree changed and the damping started to decrease, but only after about 80% of the branches were cut (Table S1).

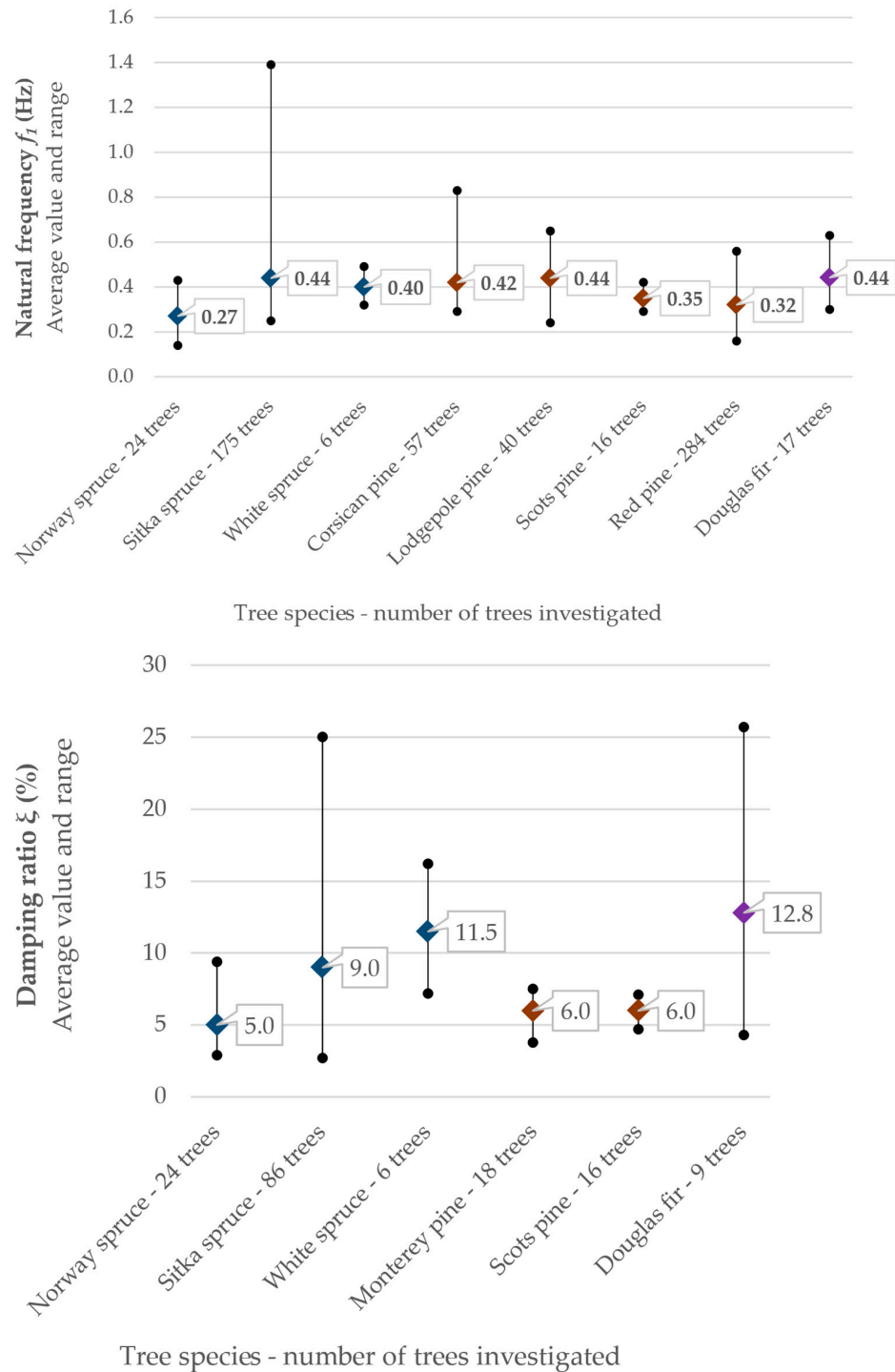


Figure 4. Natural frequency and damping ratio of conifer trees. Usage mean values are presented along with ranges, using input data from [36–41,49,50,54,55].

2.3. Morphology and Deformation Capacity

Morphology and material properties. The dynamic behavior of the trees is dominated by the size and morphology of the specimen [24]. Small morphological changes can lead to spectacular differences in the dynamic behavior of the trees [28,56]. Furthermore, different shapes of the trees are characterized by distinctive scattering of the material density, stiffness, and mass distributions [35]. Thus, the shape of the tree has more significant influence than the properties of the intrinsic material [28]. The response of the tree to the strong wind acting on the dominant direction results in lower heights of the tree [28], higher material density of the trunk on the extreme compressed fiber [57], more developed roots [58,59], larger diameter of the branches, and crowns in a flag shape [60]. At the same time, in response to wind action, changes are observed in the structure of the cell walls and in the properties of the wood [61]. Natural wood from woody plants mainly contains about 75 ÷ 80% cellulose and lignin. At the level of the cambium, the trees produce reaction wood so that the cross-section can withstand high mechanical stresses. In gymnosperms (i.e., coniferous trees), reaction wood is a compression wood type, having a high lignin content and lower cellulose content [62]. Compression wood has eccentric annual growth rings and a higher density than normal wood. Compression wood is found in the compressed fiber of trunks and branches [63], in contrast with most angiosperms, where the reaction wood is called tension wood, having an increased cellulose content of up to 60% [62,64]. Tension wood is found in the stretched fiber of trunks and branches. In porous woody angiosperms, hardwood fibers of tension wood have also been observed to produce a gelatinous cell wall layer. This gelatinous layer allows the tension wood to have greater elongations than the surrounding wood [61,65].

The Norway spruce has a macroscopic structure of a cellular solid type consisting of parallel tubes, called wood cells, that have a hierarchical internal structure [66]. The stiffness and the strength of wood are much higher along the longitudinal axis compared with directions perpendicular to it [67]. The cell wall is a fiber composite made of cellulose microfibrils embedded into a matrix of hemicelluloses and lignin (Figure 5) [68]. The matrix allows relatively large shear deformation between neighboring fibrils [69]. Cellulose fibrils wrap the tube-shaped woody cells at an angle called the cellulose microfibrils angle, γ , which varies between 0° and 90° [66].

Plastic deformation in wood. Wood is a composite material, with wood cells having a rather complicated deformation behavior, especially in large deformations [66]. In general, a typical σ - ε (normal stress-specific longitudinal strain) curve for ductile materials has an elastic slope for small strains, followed by an elastoplastic or even plastic slope for large strains. In studies on spruce, it was observed that the angle of the microfibrils decreases when the strain increases [69,70], the microfibrils reacting like a spring. At the trunk level in the stretched fiber, bending deformations produce a reduction of the angle of the microfibrils (from γ to γ') that occurs simultaneously with a shearing of the matrix between the fibrils (Figure 5). The fibrils can be considered inextensible, and the deformation takes place because of the sliding of the cellulose fibrils against each other thanks to the property of the matrix between the fibrils (Figure 5). Undeformed cellulose fibrils take up most of the load, while deformations are consumed by shearing the hemicellulose and lignin matrix. An important condition for this deformation mechanism to happen is the existence of a strong bond between the matrix and the fibrils, there being a chemical compatibility between the hemicellulose and the fibrils (both being polyoses). Hemicellulose acts as an adhesive between the cellulose fibrils and allows sliding [66].

Mechanochemical model for the deformation of hemicellulose in cell walls of coniferous wood. At the contact between hemicellulose and cellulose fibrils, a hydrogel-type matrix is formed, and it is assumed that, when the fibrils are subjected to axial stress at the fibril-matrix interface above a certain limit value of the unit shear stress (τ), the matrix shears and flows by opening and reforming hydrogen bonds. The mechanical response of the hemicellulose and lignin matrix is represented as a characteristic curve τ - η (shear stress-strain, Figure 5) [66,69,71].

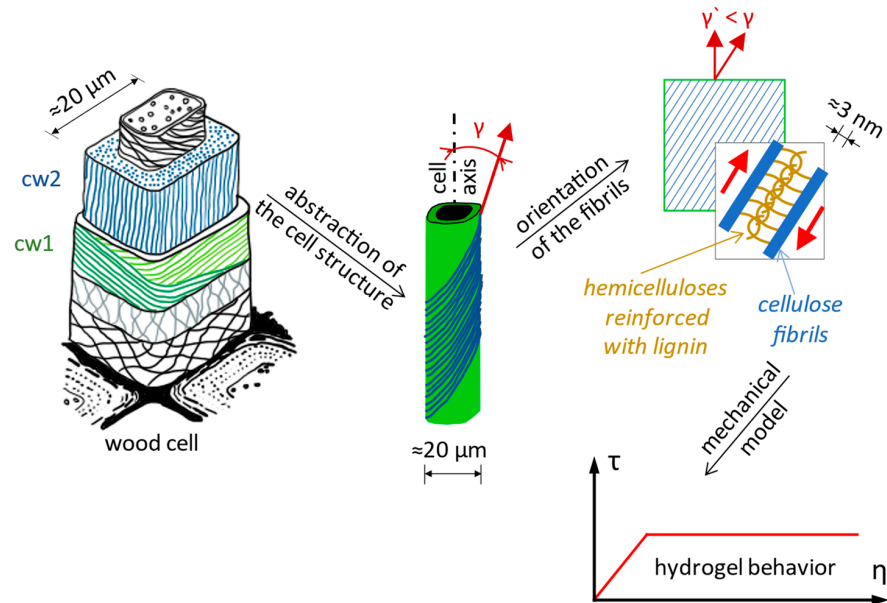


Figure 5. Cell wall structure in coniferous wood, representing the main cell walls cw1 and cw2, respectively, the middle lamella between the cells (left side), data from [68]. Geometry of cellulose microfibrils in the cell wall of coniferous wood and the angle made by the microfibrils with the longitudinal axis of the cells, γ , which decreases with increasing axial stress along the cell walls (in the center), data from [66,69,70]. The mechanical response of the cellulose fibrils embedded in the hemicellulose and lignin matrix, represented as a characteristic curve τ - η (shear stress–strain) (right corner), data from [66,69,71].

Young’s modulus. To be able to perform a modal analysis of the tree and to determine its eigenmodes and their corresponding frequency, the Euler–Bernoulli formulation may be used. In this regard, it is necessary to know the longitudinal elasticity modulus of the material and the geometric characteristics of the equivalent cantilevering beam. For about 650 trees, averages of these quantities are summarized in [72] and shown in Table 1. Given that the cellulose microfibrils remain mainly undeformed, the Young’s modulus of the material is mainly reported on their stiffness.

Table 1. Average value of green wood properties of some conifers, data from [72].

Genus/Species	Number of Trees Investigated	Modulus of Elasticity of Green Wood, E_g (GPa)	Density, ρ (kg/m ³)	The Ratio of Crown Weight to Stem Weight, W_{crown}/W_{stem}
<i>Spruce (Picea spp.)</i>				
Norway spruce (<i>Picea abies</i>)	32	6.23	598	0.32
Sitka spruce (<i>Picea sitchensis</i>)	175	7.53	447	0.50
White spruce (<i>Picea glauca</i>)	6	7.40	466	0.34
<i>Pine (Pinus spp.)</i>				
Corsican pine (<i>Pinus nigra</i>)	57	8.70	657	0.34
Lodgepole pine (<i>Pinus contorta</i>)	40	6.90	487	0.33
Scots pine (<i>Pinus sylvestris</i>)	20	7.33	700	0.29
Red pine (<i>Pinus resinosa</i>)	300	8.80	410	0.22
<i>Douglas fir (Pseudotsuga spp.)</i>				
Douglas fir (<i>Pseudotsuga menziesii</i>)	17	9.83	583	0.16

2.4. The Root System: Reaction Forces (Tree–Ground Anchorage Forces)

The root system can be regarded as a foundation system of the superstructure. However, in contrast, the root system brings together the root biomass with the related soil. Moreover, it is a living organism that grows together with the crown and the trunk. Its

mechanical performance is given by the roots' properties, the bonded soil, and the size of the system, which is variable as the cross-section decreases with the depth [9]. Figure 6 explains the four mechanisms through which the root–soil connection gives resistance to the tree base.

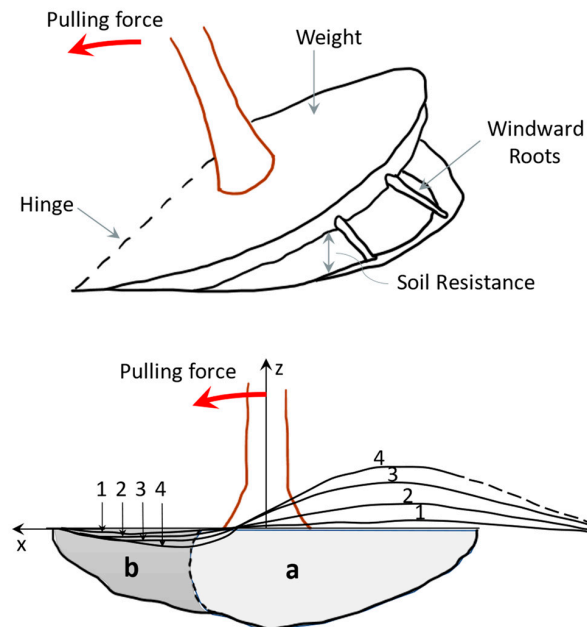


Figure 6. Diagrammatic view of a shallow-rooted tree, emphasizing the components of the anchorage (weight of the root–soil plate, soil resistance to uprooting, windward roots in tension, bending resistance of the root–soil system in the plastic hinge area) that resist the horizontal force acting on the stem. The curves 1 to 4 represent the deformation of the root–soil–plate as the pulling force grows. The area a is where the soil remains in the “elastic” domain, while in area b large deformation occurs, specific to a plastic zone. A Coutts concept adapted from [73–75].

When a horizontal force acts on the tree trunk, the weight of the roots and their associated soil help to weigh down the root–soil plate, which is the first component. The soil under and around the plate is broken during uprooting (Figure 7); consequently, the soil’s tensile strength contributes to the load-bearing capacity of the foundation (the second component). The third component is the tensile strength of the roots parallel to the direction of action of the horizontal force. And the fourth is the bending resistance of the roots and the soil around the plastic zone (area b in Figure 6) [73].

The length of the root network increases with age and can reach kilometers or even tens of kilometers [74]. The anchoring performance of the system is given by the roots that carry the tensile stresses and the adjacent soil sustaining the compression stresses. The reaction forces at the root–soil plate level depend on the following factors [9]:

- Structure and mechanical properties of the roots;
- Spatial distribution and way of anchoring of the roots;
- The structure and physical/mechanical properties of the soil, of which moisture plays an essential role;
- The interaction between the roots and the surrounding soil.

The distribution of the reaction forces into the four components is very variable due to the highly complex structure [9]. However, considering a body of rotation as a biomechanical model with the main and lateral roots generally converging in a direction towards the theoretical fixation point O_1 (Figure 8), it can be further considered that the directions of the reaction forces in the roots and their resultant forces, T (tension) and $C_{inf} + C_{lat}$ (compression), converge at the same point. It follows that, for the tree loaded with self-weight + external actions, in a stable equilibrium state, the tensile reaction forces

in the roots act on one area of the contour surfaces, and the compression from the ground reinforced with roots acts on the rest. To quantify these tree–soil connection forces, a force distribution model on the contour surfaces can be adopted. In this context, Grudnicki [9] adopts the simplified linear distribution of the reaction forces on the contour surfaces, which also facilitates the determination of the resultant forces T , C_{inf} , and C_{lat} (Figure 8).

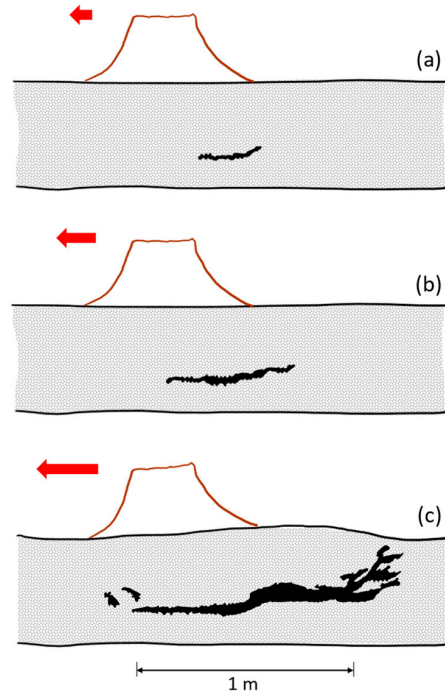


Figure 7. Sequences in root–soil system failure when a tree is pulled with an increasing horizontal force (red arrows). (a) Formation of crack close to stem base on windward side, (b) cracks extending windward and leeward, (c) appearance of cracks for the maximum uprooting turning moment, adapted from [73].

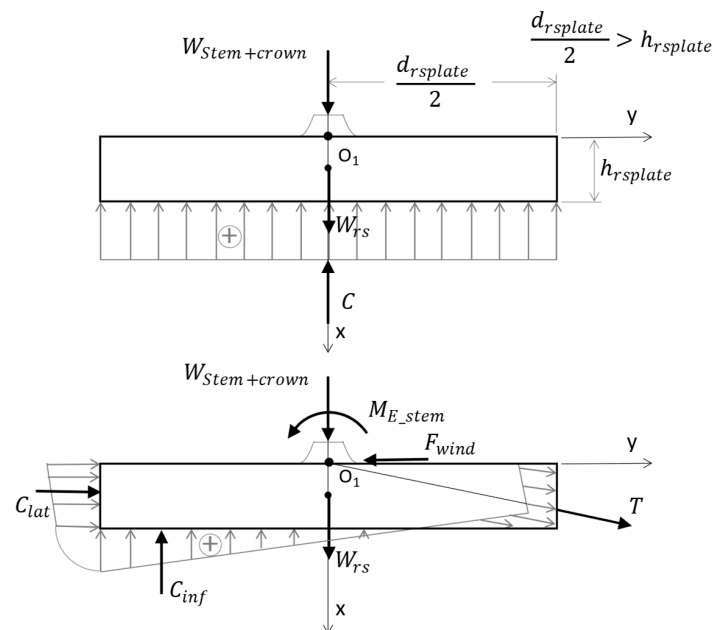


Figure 8. Distribution of reaction forces at the base of the foundation under the assumption of a centric compression (a compression with high eccentricity), a Grudnicki concept, adapted from [9]. The root–soil plate is considered to have an average diameter of $d_{rsplate}$ and a depth of $h_{rsplate}$.

2.5. Failure of Trees under Wind Action

Mayer states that no tree can withstand a violent storm and questions how to put into practice the results obtained from investigations on tree oscillations [76]. The failure mode of the trees under the dynamic action of wind is unknown to us because the real dynamic process has never been verified by field experiments on a natural scale in which all the relevant parameters have been monitored [77]. And the assumption that peak wind loading during a storm is the key factor causing degradation has never been verified in situ, and it is possible that a more important factor is root fatigue from several previous storms [77].

Studies on the impact of certain hurricanes on urban pines in Florida, USA show that failure by trunk breakage occurred mostly in *Pinus elliottii* (slash pine) trees—64% during Hurricane Jeanne—while the majority of *Pinus clausa* (sand pine) trees broke only during Hurricane Jeanne—71% [78]. Continuing with another hurricane (Ivan), here the primary failure mechanism was uprooting. Except for post-storm investigations in which the wind speed of tree failure was estimated [79], to date there are no scientific methods that can predict tree failure at a certain wind speed [24]. In Figure 9, the representative shapes of tree instability are sketched [7].

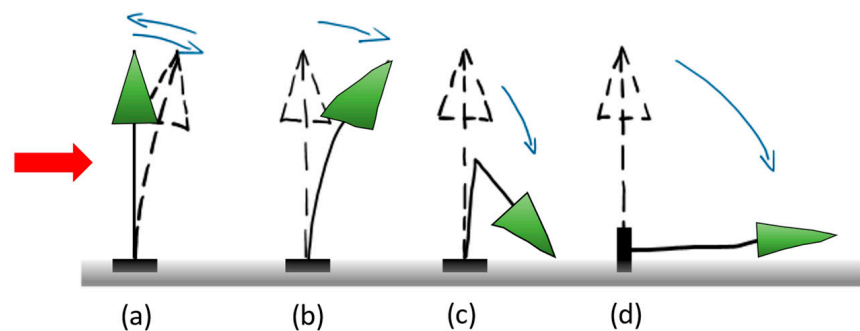


Figure 9. Shapes of tree deformability and instability due to wind action (the direction of wind is represented using the red arrow). (a) Bending and elastic buckling of the trunk, in which case the trunk returns to its original vertical position, (b) bending and plastic buckling of the trunk, in which case the stem remains deformed, (c) breakage of the trunk, and (d) overturning the tree by uprooting. Adapted from [7].

Resistance to uprooting. An approach for the assessment of uprooting resistance is to estimate the weight of the root–soil plate (foundation consisting of roots + associated soil) and then calculate the resisting bending moment at overturning [80]. The tree is uprooted if the resisting bending moment at overturning is exceeded, while this moment depends on the weight, depth, and diameter of the foundation and on the properties of the soil [43,73]. In addition to the weight of the foundation, there are other factors that can contribute to the stability of the tree foundation, such as the tensile strength of the roots parallel to the direction of the wind or the plasticizing strength of the roots and soil. Due to the complexity of the individual assessment of each individual factor, their input is introduced into Equation (3) as the coefficient A_{rsw} [80], based on tree pulling experiments from [81]. The A_{rsw} coefficient indicates the ratio between the weight of the root–soil plate and the total anchoring force of the roots in the soil [73,80].

$$M_{R_{rs}} = \frac{m_{rsplate} \cdot g \cdot h_{rsplate}}{A_{rsw}} \quad (3)$$

$$h_{rsplate} = \frac{h_{rscone}}{3} \quad (4)$$

where $M_{R_{rs}}$ is the resisting bending moment of the total root–soil plate anchorage (kN·m), $m_{rsplate}$ is the fresh mass of the root–soil plate (kg), g is the gravitational acceleration

($\text{m}\cdot\text{s}^{-2}$), and h_{rsplate} is the mean depth (m) of the root–soil plate volume (Equation (4) and Figure 10). The contribution of the root–soil plate to the total anchoring force is considered 30% for Scots pine, 20% for Norway spruce, and 30% for birch, respectively [80].

Resistance to stem breakage. If we accept the hypothesis that when the tree trunk is bent, or any cross-section of the distribution of normal stresses varies linearly, then the maximum stress values at the edge fibers decrease to zero as we approach the neutral axis [80,82]. In this hypothesis, the critical section is considered at the height $z = 1.35$ m (breast height) measured from foot to top, the trunk diameter being equal to DBH (diameter at breast height) [80]. The trunk is considered to break when the maximum stress exceeds the flexural strength for green wood, $f_{\text{fl,gw,stem}}$ [47,83,84], while the resisting bending moment to breaking the trunk (maximum turning moment a tree stem can withstand without breakage) can be calculated using Equation (5) [80,82,85].

$$M_{\text{R_stem}} = \frac{\pi \cdot \text{DBH}^3}{32} \cdot f_{\text{fl,gw,stem}} \quad (5)$$

Figure 11 shows values of resistance to overturning by uprooting and by breakage of the trunk for several Scots pine trees [86]. Analyzing the results, one can see that all trees loaded with self-weight and a lateral force failed by overturning with uprooting, the trunk bending resistance being almost four times higher than the uprooting resistance. The following data are considered in the calculations: modulus of elasticity 7000 MPa, flexural (bending) strength of the stem 32 MPa (=70% of breaking stress), fresh density of soil 1700 kg/m^3 , tree species Scots pine [86].

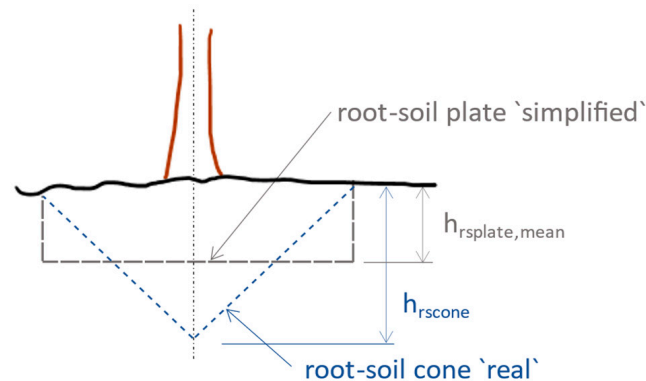


Figure 10. Root–soil plate at tree uprooting; cone and circular plate. A sketch of the concept described in [86].

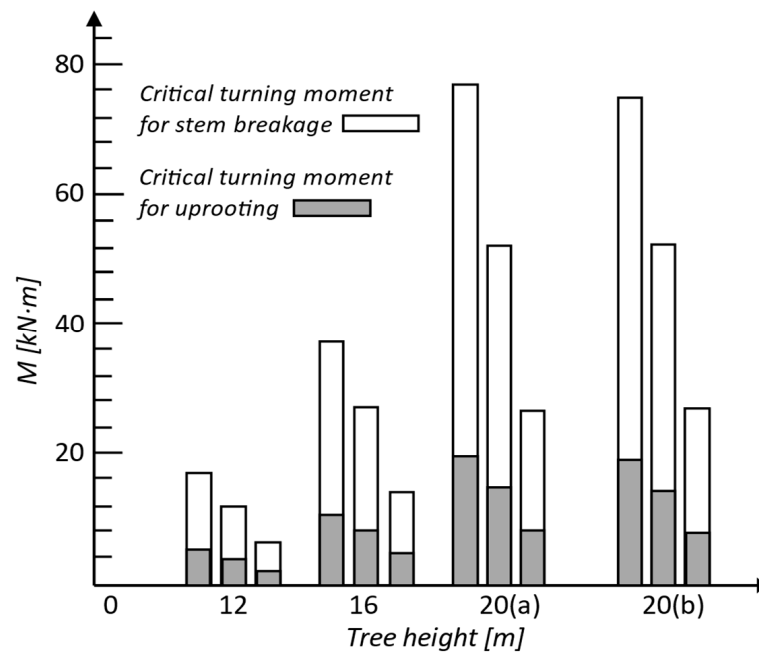


Figure 11. Turning moment needed to uproot versus turning moment needed to break the stem of Scots pine trees (crown-to-stem weight ratio (a) 0.3 and (b) 0.5). The mean ratio turning moment by gravity/turning moment by wind was less than 20%. Adapted from [86].

2.6. The Biomechanical Model of Conifers

In terms of stability, a tree can be divided [9] into:

- Elevation, consisting of stump, trunk, and crown;
- Foundation, consisting of roots and related soil, called the root–soil system.

Modeling the trunk as a beam element of variable cross-section along the length of the shaft has been shown to provide valid results in determining the natural period of vibration [72]. This solution allows the biomechanical model to consider the degree of flexibility/fixation of the trunk in the foundation.

So, a first simplified option is to consider the trunk as a cantilevered vertical beam, fully fixed at the base and with a bending stiffness adjusted according to the effective stiffness of the trunk–root–soil system. By idealization, the elevation is considered fixed in the foundation at ground level, and the root system is considered to be a reinforced foundation created by the tree [9]. The appropriate body of rotation as a biomechanical model for the root–soil system of the spruce is a cylinder or a truncated cone of shallow depth (Figure 10). To establish the distribution of self-weight and external loads, one starts from the contour curves of the spindle and the crown; in this field, there are mathematical relationships published in specialized works of dendrometry [9].

The second option consists of joining the trunk–root–soil system, consisting of the trunk modeled as a beam with a certain spring and rotation stiffness. There is a lot of information about the dynamics of fully fixed cantilevers but much less about cantilevers with semi-rigid joints. The latter situation is encountered in structural engineering, especially in the design of columns with foundations placed on soft soils. For a root–soil system of circular shape in the plane, the rotational stiffness equation can be written as for a circular plate placed on deformable soil, i.e., the Winkler foundation model (Winkler bedding coefficient/soil spring constant) [72,87,88]:

$$K = \frac{G_{rs} \cdot d_{rsplate}^4}{6 \cdot (1 - \nu_{rs-s})} \quad (6)$$

where G_{RS} is the shear modulus of the root–soil system, $d_{rsplate}$ is the diameter of the circular foundation (approximated as a mean value), and ν_{RS-S} is Poisson’s ratio of the root–soil system. This calculation approach is specific to building foundations, but here G and ν refer to the behavior of the root–soil composite material in the root–soil system.

Degree of fixation of the trunk in the foundation. Knowing the degree of fixation of the trunk in the root–soil system helps us to quantify and distinguish the flexibility of the root–soil system from stem flexibility in living trees. The stiffness of the root anchorage is influenced by the modulus of elasticity, the cross-sectional area, and the architecture of the roots, and by the physical and mechanical characteristics of the soil. Mathematically, root–soil system stiffness can be quantified using an elastic spring constant/stiffness coefficient for root–soil rotational stiffness. Thus, in [89], Equation (7) is written for the secant stiffness, k_{root} , where M_{E_stem} is the bending moment calculated at the base of the trunk, Φ_i is the rotation due to the pulling force, and Φ_0 is the initial (existing) rotation before pulling test.

$$\Phi_i = 11.9 \cdot (DBH^2 \cdot H)^{-0.53} \quad (7)$$

where Φ_i is expressed in degrees [°].

Regarding the spruce trees presented in [75], having the dimensions $DBH_A = 69$ cm and $H_A = 39$ m and $DBH_B = 16$ cm and $H_B = 16$ m, it was observed that the maximum bending moment ($M_A \approx 900$ kN·m) for the one with the thicker trunk was achieved for a rotation $\Phi_A \approx 3.5^\circ$, while, for the spruce with a thinner trunk, the maximum bending moment ($M_B \approx 11$ kN·m) was approx. 80 times smaller but reached a rotation 10 times larger ($\Phi_B \approx 26^\circ$). In [87], it was noted that root rotation contributed between 5 and 15% to the total flexibility of Sitka spruce trees.

2.7. Study Site

In Spring 2020, many coniferous trees (*Picea abies*) were downed by strong winds in the Călimani Mountains (Romania) (Figure 12). On this site, we conducted a study on an area of about 1 ha, with mainly Norway spruce vegetation ($47^\circ 09' N$, $25^\circ 48' E$, ≈ 1125 m altitude), the age being 80 years. The average annual temperature is 5.4 °C. The annual amount of annual precipitation is 926 mm at the nearest meteorological station. The soil type has been classified typical Districambosol, and the texture is brown acid. The slope of the land for the measured trees is 25 degrees, facing East.



Figure 12. Coniferous trees blown down by the wind (near Bilbor, Călimani Mountains, Eastern Carpathians, Romania).

The forest was affected by strong winds, with many trees being uprooted, broken, or left leaning (Figures S1–S30). From these, we selected 30 specimens of uprooted trees, ensuring that they had close values for diameter, height, and crown size. We measured the diameter of the trunk, the length of the stem, and the dimensions of the root system (thickness, diameters, depth, (Figure 13 and Table 2)).



Figure 13. Measured parts of a root–soil plate: orthogonal diameters ($d_{rsplate1}$ and $d_{rsplate2}$) and depth ($h_{rsplate}$ and h_{rscone}) (near Bilbor, Călimani Mountains, Eastern Carpathians, Romania). Measurement on site of the root–soil plate size and the DBH.

Table 2. Descriptive characteristics of the 30 specimens of Norway spruce investigated in the Bilbor region.

No.	Height (m)	Diameter at Base (cm)	DBH (cm)	$h_{rsplate}$ (cm)	$d_{rsplate1}$ (m)	$d_{rsplate2}$ (m)	$M_{R_{rs}}$ (kN·m)	$M_{R_{stem}}$ (kN·m)	$M_{R_{stem}}/M_{R_{rs}}$ (-)
1	29.0	41	36	25	3.4	2.7	34.2	140.2	4.1
2	29.0	42	36	30	3.5	1.8	37.2	140.2	3.8
3	28.5	38	32	27	2.3	1.6	16.3	98.4	6.0
4	30.0	43	38	34	3.4	2.4	57.3	164.8	2.9
5	30.5	45	39	29	3.2	2.0	33.5	178.2	5.3
6	31.0	51	42	30	3.5	2.4	46.1	222.6	4.8
7	30.5	50	41	26	3.4	2.5	34.7	207.0	6.0
8	30.0	43	39	29	3.2	2.1	34.8	178.2	5.1
9	27.5	36	32	20	2.0	1.4	6.8	98.4	14.5
10	29.0	40	38	24	3.0	2.3	23.8	164.8	6.9
11	29.5	41	38.5	30	3.2	2.4	41.6	171.4	4.1
12	28.0	39	37	29	3.0	1.8	28.5	152.2	5.3
13	27.0	38	34	26	2.8	1.7	20.2	118.1	5.9
14	28.0	37	32	28	2.1	1.7	16.7	98.4	5.9
15	31.0	42	38	30	2.4	2.1	26.8	164.8	6.1
16	30.0	43	38.5	30	3.1	2.2	37.2	171.4	4.6
17	29.0	36	34	28	2.2	1.7	17.6	118.1	6.7
18	28.5	41	36	30	3.0	1.8	30.5	140.2	4.6
19	29.0	40	36	27	3.3	2.5	36.1	140.2	3.9
20	30.5	41	39	34	3.5	2.6	63.3	178.2	2.8
21	30.0	48	40	30	3.4	2.6	47.7	192.3	4.0
22	31.0	50	42	26	3.6	2.7	39.5	222.6	5.6
23	27.0	35	32	25	2.2	1.6	13.3	98.4	7.4
24	27.0	37	34	28	2.7	2.0	25.5	118.1	4.6
25	30.0	40	37	32	3.2	2.2	44.0	152.2	3.5
26	28.0	36	33	30	3.1	2.0	34.5	108.0	3.1
27	30.0	50	42	34	3.4	2.2	53.4	222.6	4.2
28	30.0	48	40	27	3.1	2.6	34.9	192.3	5.5

Table 2. Cont.

No.	Height (m)	Diameter at Base (cm)	DBH (cm)	$h_{rsplate}$ (cm)	$d_{rsplate1}$ (m)	$d_{rsplate2}$ (m)	$M_{R_{rs}}$ (kN·m)	$M_{R_{stem}}$ (kN·m)	$M_{R_{stem}}/M_{R_{rs}}$ (-)
29	28.5	42	37	29	2.8	2.1	29.7	152.2	5.1
30	30.5	51	42	32	3.5	2.5	54.3	222.6	4.1

Note: the height of the tree, the diameter of the stem at the base, the diameter of the stem at breast height, and the two diameters of the root–soil system (with elliptical shape in plane) were measured on site. The thickness of the root–soil plate was evaluated with on-site measurement. The ratio $M_{R_{stem}}/M_{R_{rs}}$ was calculated considering the following estimated values based on the on-site information correlated with the bibliographic resource [80], as follows: flexural strength of the green wood in stem $f_{fl, gw, stem} = 30.6$ MPa; modulus of elasticity of green wood = 6300 MPa; crown-to-stem weight ratio = 0.50; contribution of root–soil plate weight to total anchorage $A_{rsw} = 20\%$; mean density of the fresh root–soil plate = 1500 kg/m³; mean density of green wood = 800 kg/m³. In Equation (1), for coniferous λ is considered 1.5, according to [72]. First natural frequency is calculated with Equation (1) and verified with Equation (2); in the end, same value of 0.10 Hz was obtained for all 30 specimens investigated.

The calculations made based on field investigation (Table 2) show that the $M_{R_{stem}}/M_{R_{rs}}$ (-) average ratio was 4.9 (standard deviation 2.1, with range of values between 2.8 and 14.5). The natural frequency calculated using Equation (1) and verified with (2), shows that all trees studied had almost identical dynamic characteristics, the frequency being equal to 0.10 Hz. This confirms the hypothesis that trees in the same stand have equal natural frequencies. The two calculated parameters, the $M_{R_{stem}}/M_{R_{rs}}$ ratio and the fundamental frequency (natural frequency), fall within the average values obtained from the previously cited studies. As a result, the computational relationships and assumptions used for the biomechanical model confirm an adequate abstraction of the biological model.

3. Design Methodology Transfer from Coniferous Trees to Load-Bearing Structures

In general, the design of a structure starts from an architectural concept, most of the time aesthetically motivated but not always with well-defined ideas about methods of realization and performance in relation to its function and environmental conditions. Contemporary structural engineers use general design prescriptions, building statics, seismic analysis, and other such design tools to produce an initial design (structural concept). The structural concept may be refined through an iterative process until certain prescriptive conditions are met. Questions regarding the suitability of shape, building materials, construction methods, performance objectives, cost optimization, etc., are sometimes addressed from the beginning of the design process, especially by experienced and dedicated designers. But, at other times, such questions are addressed too late to add value to the project [5].

3.1. Steps from Biomimetics to Know-How Transfer

The first step is to identify and note the characteristics of coniferous forest trees that may be applicable and associate them with the design and construction of the single-story frame structures (fully fixed columns at the base and beams with hinges at the ends). Although there are many differences between biology and structural engineering, in this study, the focus is on the similarities that can help improve the design of tall single-story structures through bioinspiration.

In step two, affinity conditions are stated based on the in-depth study from step one.

And in the third step, experimental tests are used to verify the efficiency of the mimicked property.

3.2. Step 1: Identifying the Structural Characteristics of Coniferous Forest Trees

According to the bibliographic study undertaken, the following structural characteristics of coniferous forest trees are relevant for the study of long reinforced and prestressed concrete columns [5,28,90–97]:

- Trees are three-dimensional structures statically determined;
- From the building statics' perspective, trees are vertical cantilevers;
- In a tree, the values of internal forces due to its own weight are minimal in relation to the external forces caused by wind and/or snow;
- All the elements of a tree are made of the same material, but the chemical composition, density, and mechanical properties can vary, and the load-bearing capacity varies along the element depending on the size of the applying force in that cross-section;
- Trees are believed to have a minimum mass structure with elements optimized for function and shape;
- The lack of mechanical ductility of the trees is compensated by greater flexibility and damping;
- The average fraction of the critical damping, ξ , lies between 5% and 12.8%;
- Trees maintain relatively large lateral displacements in extreme wind conditions;
- Tree joints can have a quasi-plastic response to extreme loads;
- Tree joints are endowed with a higher tenacity than that of the trunk and branches;
- Trees are systems with several degrees of freedom and with high damping;
- Trees in the same stand, although they have different heights, have the same natural frequency;
- Due to the high damping capacity and the multitude of independently vibrating elements (leaves and branches), trees rarely enter resonance;
- Tree trunks are naturally prestressed in both directions, longitudinally and circumferentially;
- Tree roots are thus designed to deform and uplift to a certain extent to prevent permanent damage to the base of the trunk.

However, it is important to mention the structural characteristics of coniferous forest trees [36–39,41,49–51,72], which differ substantially and are difficult to implement in a

single-story warehouse with long reinforced and prestressed concrete columns embedded at the base and hinged at the top. In the following, a Norway spruce tree in an arboretum is discussed in comparison with a column from a single-story warehouse, both of equal heights. The warehouse has a height of 10 m and a roof area per column of 300 m², considering the columns as having a square cross-section of 60 × 60 cm (on a site with low seismicity) and 100 × 100 cm (on a site with high seismicity). The roof is made of main and secondary roof beams of prestressed reinforced concrete, on top of which is placed a light covering made of corrugated steel sheets and a heat-insulating layer (own weight of the roof skin is 45 kg/m², technical load is 50 kg/m², and snow load is 150 kg/m²):

- The slenderness of the spruce trunk is 5 times higher than that of the columns for low seismicity regions ($a_g = 0.10$ g) and 10 times higher than that of the columns for high seismicity regions ($a_g = 0.30$ g);
- The ratio between the weight of the crown and that of the stem ($W_{\text{crown}}/W_{\text{stem}} = 0.5$) is 24 times smaller than the ratio of roof's total loads (including self-weight) and column weight ($W_{\text{roof}}/W_{\text{column}} = 12$) for areas with low seismicity and 8 times smaller ($W_{\text{roof}}/W_{\text{column}} = 4$) for areas with high seismicity;
- The natural period of vibration for trees is between 10.0 and 2.0 s, while for a single-story warehouse it is between 2.3 and 0.7 s;
- The alternation of synchronous and asynchronous oscillations of the branches with the effect of dissipating the energy induced by wind or earthquake actions contrast with the movement of the roof beams connected to the column;
- The root system is a hybrid between a shallow and a deep foundation (with individual footing and ground anchors), while for reinforced concrete columns such a solution would be too expensive, being used especially for special structures such as towers for wind turbines. In general, nowadays, the common solutions used for the foundations of the columns in single-story warehouses are either a shallow foundation as individual footing or a deep foundation with individual footing sitting on piles.

4. Features of the Biological Role Model Meant to Be Abstracted and Later Transferred

Establishing the affinity conditions is the second step in the biomimetic design. If we start from the assumption that nature can be seen as a textbook for engineers and we consider the principles of structural design, to understand and transfer the design knowledge from a living tree to an engineering structure, for example, a single-story frame structure with columns as vertical cantilevers, the following affinity conditions must be met [5,98,99]:

- Structural applicability (geometric similarities and use and behavior of materials);
- Functional similarity (similar loading conditions and similar climatic actions);
- Similar structural response (behaving in the same way under comparable external actions);
- Cost efficient (being as profitable as possible in terms of material and energy consumption and production costs).

The chosen biological role model is the Norway spruce, and the features meant to be replicated in bioinspired long reinforced concrete columns with respect to the affinity criteria are:

- At the macro-level, longitudinal prestressing for gaining increased flexural stiffness and self-centering capacity (Figure 14). The technical implementation consists in using prestressed unbonded steel strands inside the reinforced concrete column;
- At the meso-level, viscoelastic damping through sliding of the cellulose fibrils with shearing of the hemicellulose and lignin matrix between them (Figure 15). The technical implementation is solved by greatly upscaling the fibrils (diameter of ≈ 3 nm) embedded into a matrix of hemicellulose and lignin and substituting them with steel strands (diameter of ≈ 9 mm) embodied in a concrete mixture with lignin and hemi-

cellulose content. Thus, it targets a controlled bond slip of the steel strands when in tension or in compression.

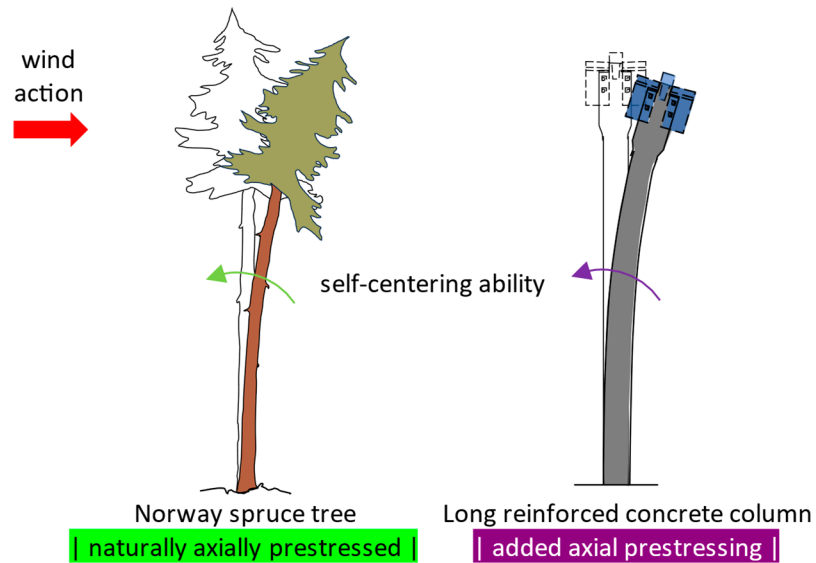


Figure 14. Deformed Norway spruce tree under wind loads, and deformed reinforced prestressed concrete column due to a horizontal point load at the top.

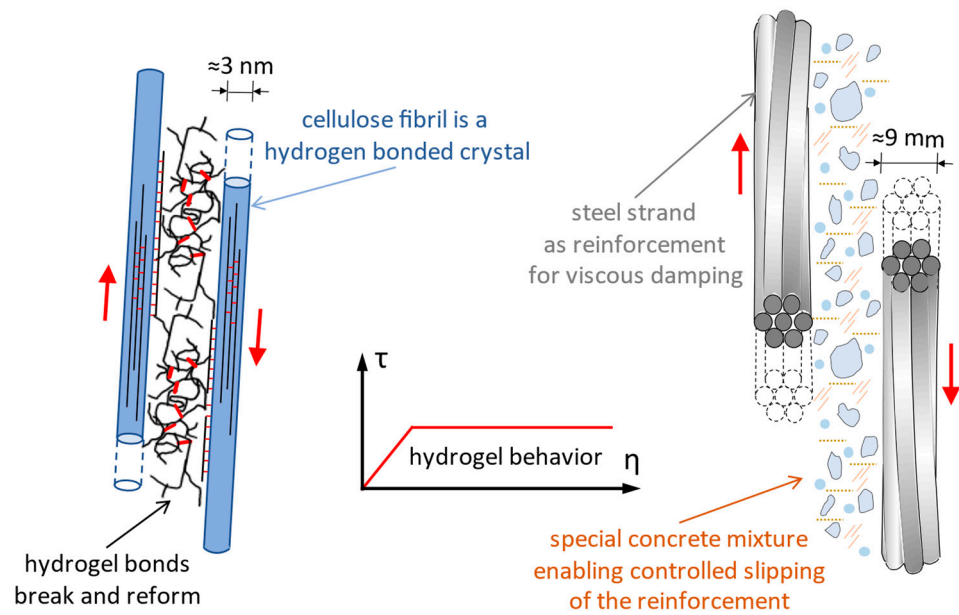


Figure 15. Deformation of cellulose fibril and of hemicellulose-lignin based matrix in cell walls of Norway spruce wood, and deformation of steel strands inside a concrete member when controlled bond slip of reinforcement is enabled. The red arrow represents the direction of the axial force inside of the fibril, respectively inside of the steel strand.

5. Results and Discussion

Step 3 presents the design and testing of bioinspired structural concrete, first at the macro-level (a reinforced concrete column centrally prestressed) and second at the meso-level (characterization of reinforcement bond in concrete in the presence of lignin).

5.1. Experimental Study on the Influence of Centric Prestressing in Long Reinforced Concrete Columns

Chirițescu and Kiss carried out an experimental study on long prestressed and reinforced concrete columns in order to determine the influence of centric prestressing on the bending stiffness and energy dissipation capacity of concrete columns [100–102]. The study consisted of physical experiments and numerical simulations on columns with a cross-section of 250×250 mm (Figure 16), tested as cantilever elements with a length of 3.2 m and two forces concentrated at the top (W_{ext} , the equivalent axial force due to roof's self-weight of the warehouse; F_{lat} , the equivalent lateral force caused by wind action and seismic action) (Figure 17). The materials used for series S01 were concrete C60/75 and reinforcing steel/passive reinforcement B500C, while series S02 is like S01 except that approx. 60% of the passive reinforcement area was replaced by prestressing steel/active reinforcement Y1860S7, so that the resisting bending moments for the two cross-sections were equal (Table 3). Column S02 was centrically prestressed in the longitudinal direction with a P_0 force, resulting in a mean precompression stress of approx. 5.6 MPa.

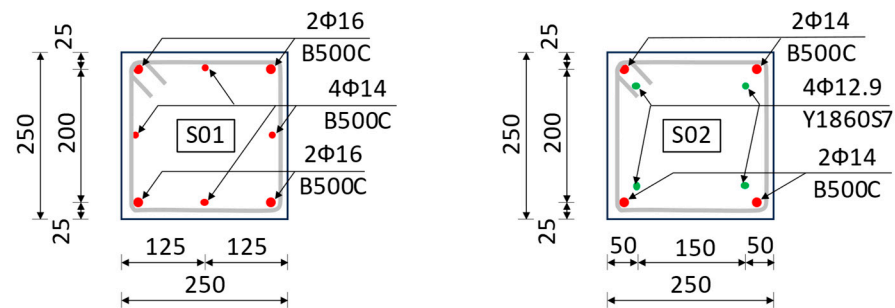


Figure 16. Cross-sections of S01 and S02, dimensions in mm. Adapted from [100].

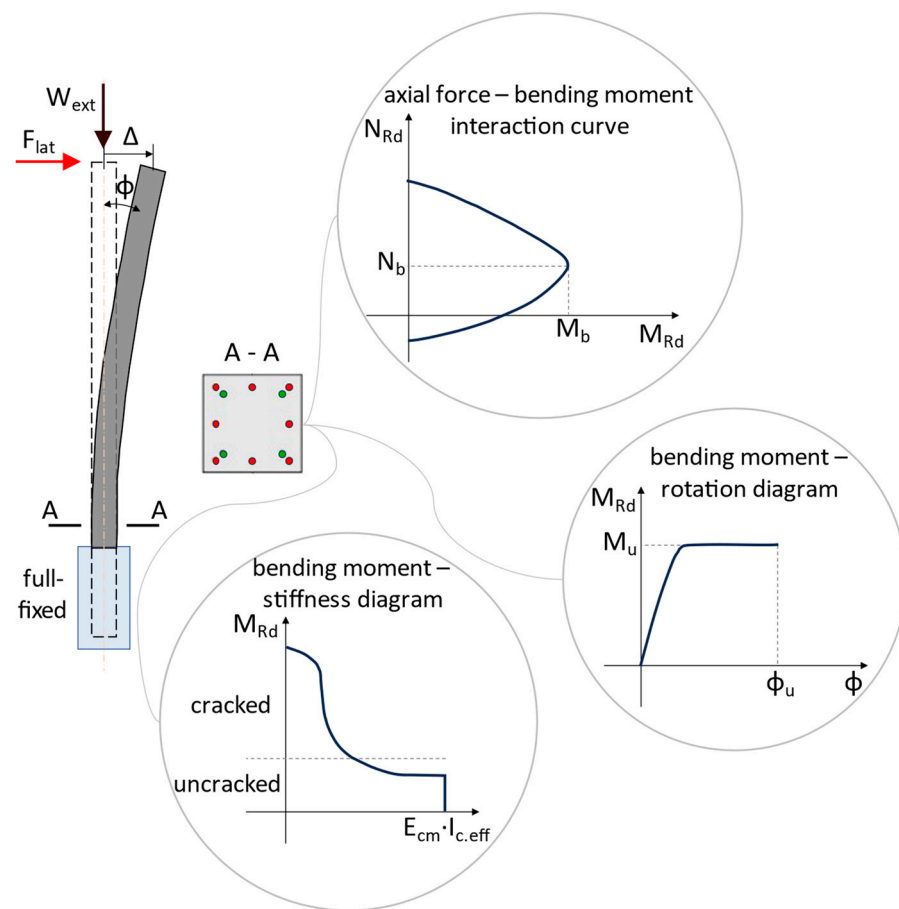


Figure 17. Sketch with test set-up and analyses of prestressed concrete columns. Green dots represent the active reinforcement, red dots the passive one. Adapted from [103].

Table 3. Mechanical properties of used materials, data from [100].

	Modulus of Elasticity MPa	Characteristic Strength (f_{ck} , f_{pk} , f_{yk}) MPa	Ultimate Strain (ϵ_{cu} , ϵ_{pu} , ϵ_{su}) [-]
Concrete C60/75	39,000	60	0.3%
Prestressing steel Y1860S7	199,000	1860	2.2%
Reinforcement B500C	205,000	500	7.5%

As a result of the experimental tests in the laboratory, the following were found:

- For the same lateral force of 24 kN (approx. 80% of the failure force), the reinforced concrete column (S01) had an average lateral displacement of 426 mm ($\approx 13.3\%$ drift) compared with the prestressed reinforced concrete column (S02), which had an average lateral displacement of 289 mm ($\approx 9.0\%$ drift), which means an increase in stiffness of almost 50%;
- Section S02 was less ductile than S01, the energy dissipation capacity being reduced by about 40%. This was caused by the much lower ultimate elongation of the prestressing steel (2.2%) than that of the reinforcing steel (7.5%), collaborated with the uninterrupted adhesion (full bond) of the active reinforcement along the entire length of the column;
- The prestressed elements had self-centering capacity;

- The use of centrally prestressed reinforced concrete columns for single-story warehouses was efficient to reduce lateral displacements at the top of the building (through longitudinal prestressing, the bending stiffness associated with large bending moments was reduced, Figure 17). Cracking of the concrete occurred much later compared with reinforced concrete members without prestressing but, at the same time, a reduced value of the behavior factor must be considered in the seismic design depending on the displacement ductility factor ($\mu_\delta = \Delta_u / \Delta_c$) and on the real curvature ductility factor ($\mu_\theta = \phi_u / \phi_c$) of the cross-section.

5.2. Experimental Study on the Influence of the Walnut Shell on the Bond of the Reinforcement in Concrete

In this study, it was aimed to mimic the viscoelastic damping of coniferous trees during wind action. When their trunks bend and the cellulose microfibrils wrapped along the wood cells allow the trunk and branches to bend by shearing the hemicellulose and lignin matrix, the microfibrils remain inextensible. In the case of reinforced concrete columns, flexural deformation occurs because of cracking of the concrete and elongation of the steel reinforcement in the tension fiber of the cross-section. At high stresses, the reinforcement is stretched beyond the elastic limit and yields, with a strain at maximum force of minimum 7.5% (reinforcing steel of ductility class C). But, when prestressing steel is used (such as strands), the strain at maximum force is only 2.2% [100,104]. To increase the deformation capacity of the prestressed concrete elements (implicitly the energy dissipation capacity), new solutions are needed; in this case, a biomimetic approach is used. It is desired to increase the deformation capacity of concrete columns reinforced with steel strands not by elongation of the reinforcement but by controlled slipping of the strands. The technical implementation aims to obtain the hydrogel behavior of the strand-type reinforcement embedded in concrete. To obtain this result, an experimental study was carried out on the bond of seven-wire strand prestressing steel (Y1860S7), having a total diameter of 9 mm, centrally embedded in a standard concrete specimen (cube with side 100 mm, without transversal reinforcement) for a pull-out test (Figure 18 and Figures S32–S38; Videos S1 and S2).

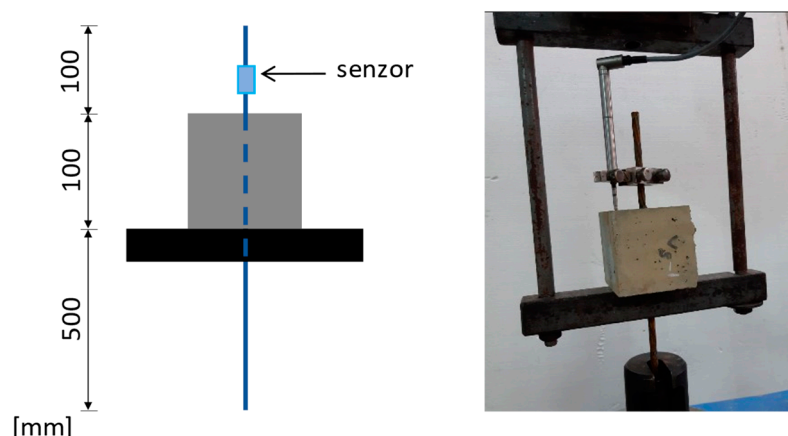


Figure 18. Sketch (not at scale) and photo with test set-up for reinforcement bond with concrete.

To establish the effect of lignin and hemicellulose on the reinforcement bond in concrete, a parametric study was carried out on concrete compositions of minimum class C30/37. The concrete class was chosen in accordance with the good execution practice of prestressed reinforced concrete elements (monolithic and prefabricated). For specimen V3, the concrete strength class obtained was C32/40, and for specimens V4, V5, and V6, C35/40 (Table 4). The parameters considered were lignin and hemicellulose, as lignosulfonate-based admixture (activated in the plasticizer, in V4), as additive of non-activated lignin and hemicellulose in the form of peanut shell powder (V5), and as additive of non-activated

lignin and hemicellulose in the form of walnut shell powder (Figure 19) (V6). The dosage used was about 1% of the amount of binder (cement). The chemical compositions of peanut shell and walnut shell are noted in Table 5. The reference specimens (V3) were made of concrete without additives and admixtures.

Table 4. Results of the pull-out tests.

Specimen	Concrete Grade	Maximum Value of Pull-Out Force kN	Average Value for Maximum Force kN
V3	V3-1	21.39	19.88
	V3-2	21.9	
	V3-3	16.35	
V4	V4-1	16.98	17.43
	V4-2	16.92	
	V4-3	18.39	
V5	V5-1	15.33	17.2
	V5-2	18.81	
	V5-3	17.46	
V6	V6-1	14.25	12.06
	V6-2	N/A	
	V6-3	9.87	



Figure 19. Walnut shell before and after fine grinding [105]. Reproduced with permission from Daria Rozian “Influența ligninei asupra rezistenței la compresiune a betonului și asupra aderenței armăturii în beton” (Master Dissertation), advisor: T.-N. Toader, UTCN, 2022.

Table 5. Chemical composition of peanut shell and walnut shell.

Compound	Walnut Shell [106]	Peanut Shell [107]
Ash	3.4%	3.8%
Lignin	50.3%	36.1%
Hemicellulose	22.4%	5.6%
Cellulose	23.9%	44.8%

It was observed that, for specimen V6 (with lignosulfonate-based plasticizer admixture + hemicellulose and lignin additive in the form of walnut shell powder), the pull-out force–slip curve for the strand embedded in concrete had the allure of the shear stress–strain curve for cellulose microfibrils wrapped in the hemicellulose and lignin matrix (Figures 20, S39 and S40). The hydrogel-like mechanical behavior may be due to the walnut shell powder acting as a glue between strand and concrete. But, to demonstrate this action, microscopic studies should be carried out to find out exactly how the powder reacts in the composition of the concrete and the chemical bond at the concrete–strand interface. The concrete mixture used for the V6 specimens is noted in Table 6.

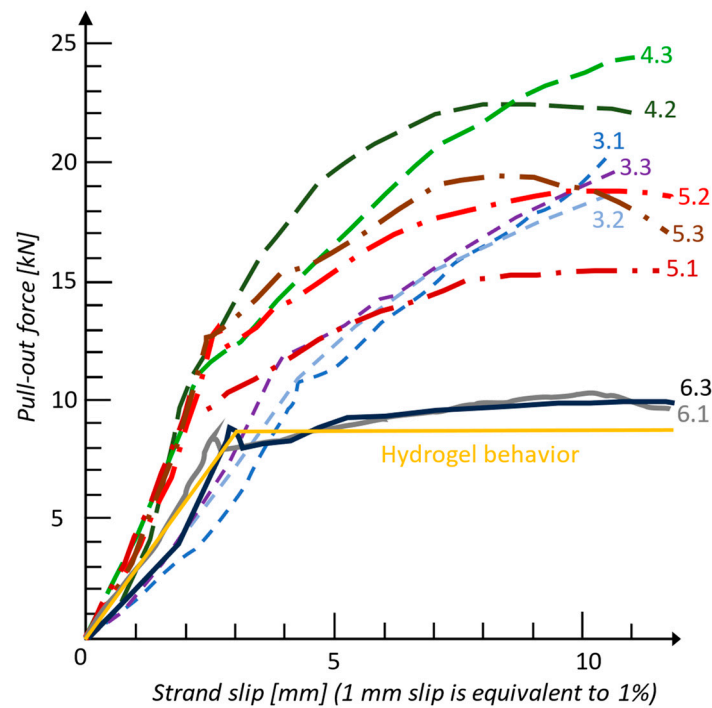


Figure 20. Force–slip curve for minimum 10% slip, obtained experimentally.

Table 6. Concrete ingredients used to obtain 3.3 L of fresh concrete (grade C35/45) to cast specimen V6.

Ingredient	Type	Amount
CEM I 52.5R	Cement	1155 g
Water	Water	533 g
Dry aggregates	Source: river	
Sand	0–2 mm	2767 g
Fine gravel	2–8 mm	1320 g
Medium gravel	8–16 mm	1921 g
Sika Plastiment BV 440	Plasticizer (lignosulfonate based)	13.3 g
Walnut (<i>Juglans regia</i>) shell powder	0.063–0.125 mm	11.5 g

Although specimens V3, V4, and V5 had a maximum pull-out force approximately 40% higher than V6, none of them showed hydrogel behavior up to 10% strand slips in concrete. The results of the study from [105] indicate the potential of using steel strands as reinforcement in concrete elements with the addition of lignin and hemicellulose to achieve a viscoelastic damping. This behavior could be exploited in the direction of increasing the deformation capacity of prestressed concrete elements (with bonded strands), for example, for dissipative zones/potential plastic hinge regions of structural concrete members in structures designed for earthquake resistance.

6. Conclusions

Finally, we can write down the bioinspired means with the greatest potential to improve the structural performance of single-story buildings with long reinforced prestressed concrete columns [5,103–105,108–114]:

- Reaching viscoelastic damping is assured by using concrete with the addition of hemicellulose and lignin and/or some longitudinal reinforcements with an integrated friction mechanism along their length;
- Supplementary damping results from the interaction of the soil foundation, such as the controlled uplifting of the foundation (solution studied on onshore concrete towers for wind turbines);

- The fraction of critical damping in coniferous trees is in the same range of that in reinforced concrete structures, so $\xi = 5\%$ is the conventional value in the design rules [115,116], which can be increased up to 20% if additional dissipative elements are introduced;
- Centric longitudinal unbonded post-tensioning of the concrete columns increases bending stiffness and enables self-centering capacity;
- Designing the structures of neighboring buildings so that the natural frequency of each is equal (this way the seismic joints will have a minimum width), as revealed by the on-site measurements of the Norway spruce trees in the Bilbor region.

Further investigations to enhance the similarity between Norway spruce trees and prestressed reinforced concrete columns will include:

- Additional studies on transversal prestressing of columns to increase the degree of concrete core confinement and the rotation capacity at the base of the column;
- Experimental tests for evaluating the viscoelastic damping after cyclic loading and unloading;
- Durability and ageing tests on the special concrete mixture containing biomass (lignin and hemicelluloses);
- Checking the hydrogel behavior on cracked concrete samples;
- Full scale experiments on concrete columns integrating both mimicked features: self-centering ability and viscoelastic damping, with bonded and unbonded strands at the same time.

Supplementary Materials: The following supporting information can be downloaded at: https://drive.google.com/drive/folders/1wZOINJXlsowtu3uB3NgDgQckPTselVxY?usp=drive_link, Figures S1–S29: *Picea abies* trees blown by the wind in Bilbor; Figure S30: Prepared samples for compression test; Figure S31: Prepared samples for pull-out test (axonometric view); Figure S32: Prepared samples for pull-out test (top view); Figure S33: Machine used for the pull-out test; Figure S34: Anchorage device for the strand in the testing machine; Figure S35: Data acquisition for pull-out test; Figure S36: Sample 3.2 after pull-out test (global view); Figure S37: Short end of the strand in Sample 3.2 after pull-out test (global view); Figure S38: Long end of the strand in Sample 3.2 after pull-out test; Figure S39: Concrete cube for strand embedding after splitting (axonometric view); Figure S40: Concrete cube for strand embedding after splitting (top view); Table S1: The natural frequency and damping ratio of conifer trees. A literature review; Video S1: Pull-out test for sample 3.1; Video S2: Pull-out test for sample 4.1.

Author Contributions: Conceptualization, T.-N.T. and C.G.-R.M.; methodology, all authors; software, T.-N.T.; validation, C.G.-R.M., H.C. and T.-N.T.; investigation, A.M.T., T.-N.T. and H.C.; data curation, H.C.; writing—original draft preparation, T.-N.T.; writing—review and editing, all authors.; visualization, all authors; supervision, C.G.-R.M. All authors have read and agreed to the published version of the manuscript.

Funding: This research received no external funding.

Institutional Review Board Statement: Not applicable.

Data Availability Statement: The data that support the findings of this study are available from the corresponding author upon reasonable request.

Acknowledgments: The authors express their special thanks to Liviu Holonec for the useful introduction into the morphology and physiology of coniferous trees. Also, the authors are thankful to Andrei Faur for his remarks concerning the hypotheses considered for passive energy dissipation in trees and concrete columns. The preparation of the Master thesis authored by Bela Kovacs and Daria Paraschiva Rozian was valuable input for validating some of the initial assumptions. Besides, the sample preparation, the mechanical tests, and the numerical simulations were carried out in the facilities of the Technical University of Cluj-Napoca, for which the authors need to be thankful.

Conflicts of Interest: The authors declare no conflicts of interest.

References

1. Kiss, Z. Îmbinări Rigide Pentru Structuri în Cadre din Beton Armat, Amplasate în Zone Seismice. *Rev. AICPS* **2018**, 126–141. Available online: <https://www.revistaconstructiilor.eu/index.php/2018/07/01/imbinari-rigide-pentru-structuri-in-cadre-din-beton-armat-amplasate-in-zone-seismice/> (accessed on 6 January 2022).
2. Kiss, Z.; Balint, K.; Mocsary, B.; Toader, N. Soluții de Fundare and Tipuri de Infrastructuri Pentru Clădiri din Beton Armat and Precomprimat. *Rev. Română Geotehnică Fundații* **2013**, 1, 29–32. Available online: <https://srgf.ro/wp-content/uploads/2022/01/RRGF-2013-1.pdf> (accessed on 6 January 2022).
3. Toader, N.; Sobek, W.; Nickel, K.G. Energy Absorption in Functionally Graded Concrete. *J. Bionic Eng.* **2017**, 14, 369–378. [CrossRef]
4. Klang, K.; Bauer, G.; Toader, N.; Lauer, C.; Termin, K.; Schmier, S.; Kovaleva, D.; Haase, W.; Berthold, C.; Nickel, K.G.; et al. (Chapter 7) Plants and Animals as Source of Inspiration for Energy Dissipation in Load Bearing Systems and Facades. In *Biomimetic Research for Architecture and Building Construction. Biologically-Inspired Systems*; Springer: Berlin/Heidelberg, Germany, 2016; pp. 109–133. [CrossRef]
5. Grigorian, M. Biomimicry and theory of structures-design methodology transfer from trees to moment frames. *J. Bionic Eng.* **2014**, 11, 638–648. [CrossRef]
6. Grudnicki, F. *Bazele Stabilității Arborilor Forestieri (“The Basis of Stability of Forest Trees”)*; Editura Universității “Ștefan cel Mare”: Suceava, Romania, 2003.
7. Grudnicki, F. Coeficientul de Zveltețe și Stabilitatea Individuală a Arborilor de Molid. *Bucov. For.* **2004**, 12, 75–87. Available online: [http://bucovina-forestiera.ro/BF%20old%20site/Bucovina%20forestiera/www.bucovina-forestiera.ro/arhiva/2004/12\(1-2\)/coeficientul-de-zveltețe-si-stabilitatea-individuala-a-arborilor-de-molid.pdf](http://bucovina-forestiera.ro/BF%20old%20site/Bucovina%20forestiera/www.bucovina-forestiera.ro/arhiva/2004/12(1-2)/coeficientul-de-zveltețe-si-stabilitatea-individuala-a-arborilor-de-molid.pdf) (accessed on 6 January 2022).
8. Grudnicki, F. Contribuții la Biomecanica Formei Arborilor (Contributions to the Biomechanics of Tree Shape). *Analele Univ. “Ștefan Cel Mare” Suceava Ser. Silvicultură* **1994**, 1, 39–48.
9. Grudnicki, F. Stabilitatea Molizilor la Acțiunea Vântului (“The Stability of Norway Spruce to Wind Action”). *Analele Univ. “Ștefan Cel Mare” Suceava. Secțiunea Silvicultură. Ser. Nouă* **2004**, 1, 23–36. Available online: http://www.silvic.usv.ro/anale/as_2004_1/as_grudnicki_2004_1.pdf (accessed on 6 January 2022).
10. Comitetul European de Standardizare, Proiectarea Structurilor de Beton. *Partea 1-1: Reguli Generale and Reguli Pentru Clădiri*; Asociația de Standardizare din România (ASRO): Bruxelles, Belgium, 2004.
11. Emil, M. *Berechnung von Eingespannten Gewölben*; Rascher: Zürich, Switzerland, 1907.
12. Emil, M. *Bemessungstabellen für das Entwerfen von Eisenbetonbauten*; Wittwer: Stuttgart, Germany, 1938.
13. Fritz, L. *Vorlesungen über Massivbau. Teil 1 mit Eduard Mönning: Grundlagen zur Bemessung im Stahlbetonbau*, 3rd ed.; Springer: Berlin/Heidelberg, Germany, 1984.
14. Fritz, L. *Vorlesungen über Massivbau. Teil 2 mit Eduard Mönning: Sonderfälle der Bemessung im Stahlbetonbau*, 3rd ed.; Springer: Berlin/Heidelberg, Germany, 1986.
15. Fritz, L. *Vorlesungen über Massivbau. Teil 3 mit Eduard Mönning: Grundlagen zum Bewehren im Stahlbetonbau*; Springer: Berlin/Heidelberg, Germany, 1977.
16. Fritz, L. *Vorlesungen über Massivbau. Teil 4: Nachweis der Gebrauchsfähigkeit: Rissebeschränkung, Formänderungen, Momentenumlagerung u. Bruchlinientheorie im Stahlbetonbau*, 2nd ed.; Springer: Berlin/Heidelberg, Germany, 1978.
17. Freyssinet, E. *Une Révolution Dans la Technique du Béton*; Eyrolles: Paris, France, 1936.
18. Fritz, L. *Teil 5: Spannbeton*; Springer: Berlin/Heidelberg, Germany, 1980.
19. Toader, T.-N.; Kiss, Z.; Țere, S.-G.; Puskás, A. An Analytical Design Approach for Post-Tensioned Concrete Slabs with Unguided Tendons. In Proceedings of the Computational Civil Engineering Empower the Digital Transition in the Construction World, Iași, Romania, 27–29 May 2021. Available online: <https://iopscience.iop.org/article/10.1088/1757-899X/1141/1/012013> (accessed on 6 January 2022).
20. Toader, N.; Haase, W.; Sobek, W. Energy Absorption in Functionally Graded Concrete under Compression. *Bul. Institutului Politeh. Iasi—Secția Construcții Arhit.* **2018**, 64, 9–23. Available online: <http://www.bipcons.ce.tuiasi.ro/Content/ArticleInformation.php?ArticleID=654> (accessed on 6 January 2022).
21. Nickel, K.G.; Klang, K.L.C.; Toader, N.; Sobek, W. The potential of improving building construction materials by a biomimetic approach. In Proceedings of the 10th International Conference on Emerging Materials and Nanotechnology, Vancouver, BC, Canada, 27–29 July 2017. [CrossRef]
22. Jan, K.; Ulrich, S.; Thomas, S. *Baubionik—Biologie Beflügelt Architektur. Subcapitolul: Gradientenbeton*; Naturkunde Museum Stuttgart: Stuttgart, Germany, 2017.
23. de Langre, E. Effects of wind on plants. *Annu. Rev. Fluid Mech.* **2008**, 40, 141–168. [CrossRef]
24. James, K.R.; Dahle, G.A.; Grabosky, J.; Kane, B.; Detter, A. Tree Biomechanics Literature Review: Dynamics. *Arboric. Urban For.* **2014**, 40, 1–15. [CrossRef]
25. Spatz, H.C.; Brüchert, F. Basic biomechanics of self-supporting plants: Wind and gravitational loads on a Norway spruce tree. *For. Ecol. Manag.* **2000**, 135, 33–44. [CrossRef]

26. Vogel, S. Blowing in the Wind: Storm-Resisting Features of the Design of Trees. *J. Arboric.* **1996**, *22*, 92–98. Available online: <https://joa.isa-arbor.com/request.asp?JournalID=1&ArticleID=2715&Type=2> (accessed on 6 January 2022). [CrossRef]
27. Miller, L. Structural Dynamics and Resonance in Plants with Nonlinear Stiffness. *J. Theor. Biol.* **2005**, *234*, 511–524. [CrossRef] [PubMed]
28. James, K.R.; Moore, J.R.; Slater, D.; Dahle, G. Tree biomechanics. *CAB Rev.* **2017**, *12*, 1–11. [CrossRef]
29. Niklas, K.J. *Plant Biomechanics: An Engineering Approach to Plant Form and Function*; University of Chicago Press: Chicago, IL, USA, 1992.
30. Lindström, H.; Evans, J.; Verril, S. Influence of Cambial Age and Growth Condition on Microfibril Angle in Young Norway Spruce [*Picea abies* (L.) Karst]. *Holzforforschung* **1998**, *52*, 573–581. Available online: <https://www.fpl.fs.usda.gov/documnts/pdf1998/linds98a.pdf> (accessed on 6 January 2022). [CrossRef]
31. Lichtenegger, H.; Reiterer, A.; Stanzl-Tscheegg, S.; Fratzl, P. Variation of cellulose microfibril angles in softwoods and hardwoods—A possible strategy of mechanical optimization. *J. Struct. Biol.* **1999**, *128*, 257–269. [CrossRef] [PubMed]
32. Reiterer, A.; Lichtenegger, H.; Tscheegg, S.; Fratzl, P. Experimental evidence for a mechanical function of the cellulose microfibril angle in wood cell walls. *Philos. Mag. A* **1999**, *79*, 2173–2184. [CrossRef]
33. Brüchert, F.; Becker, F.; Speck, T. The mechanics of Norway Spruce [*Picea abies* (L.) Karst]: Mechanical properties of standing trees from different thinning regimes. *For. Ecol. Manag.* **2000**, *135*, 45–62. [CrossRef]
34. Lundström, T.; Stoffel, M.; Stöckli, V. Fresh-Stem Bending of Silver Fir and Norway Spruce. *Tree Physiol.* **2008**, *28*, 355–366. Available online: <https://academic.oup.com/treephys/article-pdf/28/3/355/4659859/28-3-355.pdf> (accessed on 6 January 2022). [CrossRef] [PubMed]
35. Speck, T.; Burgert, I. Plant Stems: Functional Design and Mechanics. *Annu. Rev. Mater. Res.* **2011**, *41*, 169–193. [CrossRef]
36. Moore, J.R.; Maguire, D.A. Natural sway frequencies and damping ratios of trees: Concepts, review and synthesis of previous studies. *Trees—Struct. Funct.* **2004**, *18*, 195–203. [CrossRef]
37. Milne, R. Dynamics of swaying *Picea sitchensis*. *Tree Physiol.* **1991**, *9*, 383–399. [CrossRef]
38. Flesch, T.; Wilson, J.D. Wind and remnant tree sway in forest cutblocks. II. Relating measured tree sway to wind statistics. *Agric. For. Meteorol.* **1999**, *93*, 243–258. [CrossRef]
39. Jonsson, M.J.; Foetzki, A.; Kalberer, M.; Lundström, T.; Ammann, W.; Stöckli, V. Natural frequencies and damping ratios of Norway spruce (*Picea abies* (L.) Karst) growing on subalpine forested slopes. *Trees* **2007**, *21*, 541–548. [CrossRef]
40. Mayhead, G.J. Sway Periods of Forest Trees. *Scott. For.* **1973**, *27*, 19–23. Available online: <https://link.springer.com/article/10.1007/BF00123529> (accessed on 6 January 2022).
41. Mayhead, G.J.; Gardiner, J.B.H.; Durrant, D.W. *A Report on the Physical Properties of Conifers in Relation to Plantation Stability*; Research and Development Branch: Edinburgh, Scotland, 1975.
42. Holbo, H.R.; Corbett, T.C.; Horton, P.J. Aeromechanical behaviour of selected Douglas-fir. *Agric. Meteorol.* **1980**, *21*, 81–91. [CrossRef]
43. Peltola, H.; Kellomäki, S.; Hassinen, A.; Lemmittenen, M.; Aho, J. Swaying of trees as caused by wind: Analysis of field measurements. *Silva Fenn.* **1993**, *27*, 113–126. [CrossRef]
44. Hassinen, A.; Lemmittenen, M.; Peltola, H.; Kellomäki, S.; Gardiner, B. A prism-based system for monitoring the swaying of trees under wind loading. *Agric. For. Meteorol.* **1998**, *90*, 187–194. [CrossRef]
45. Petty, J.A.; Swain, C. Factors influencing stem breakage of conifers in high winds. *Forestry* **1985**, *58*, 75–84. [CrossRef]
46. Scannell, B. Quantification of the Interactive Motions of the Atmospheric Surface Layer and a Conifer Canopy. Ph.D. Thesis, Cranfield Institute of Technology, Bedford, UK, 1984.
47. Blevins, R. *Formulas for Natural Frequency and Mode Shape*; Van Nostrand Reinhold Co.: New York, NY, USA, 1979.
48. Spatz, H.-C.; Theckes, B. Oscillation damping in trees. *Plant Sci.* **2013**, *207*, 66–71. [CrossRef] [PubMed]
49. Moore, J.R.; Maguire, D.A. Natural sway frequencies and damping ratios of trees: Influence of crown structure. *Trees* **2005**, *19*, 363–373. [CrossRef]
50. Blackburn, P.; Miller, K.F.; Petty, J.A. An assessment of the static and dynamic factors involved in windthrow. *Forestry* **1988**, *61*, 29–43. [CrossRef]
51. Gardiner, B.A. Mathematical modelling of the static and dynamic characteristics of plantation trees. In *Mathematical Modelling of Forest Ecosystems*; Franke, J., Roeder, A., Eds.; Sauerlander’s Verlag: Frankfurt am Main, Germany, 1992; pp. 40–61.
52. Gardiner, B.A.; Stacey, G.R.; Belcher, R.E.; Wood, C.J. Field and wind tunnel assessments and the implications of respacing and thinning for tree stability. *Forestry* **1997**, *70*, 233–252. [CrossRef]
53. Sugden, M.J. Tree sway period—A possible new parameter for crown classification and stand competition. *For. Chron.* **1962**, *38*, 336–344. [CrossRef]
54. Loo, S.P. Aerodynamic Characteristics of a Flexible Structure (Tree). Master’s Thesis, University of Canterbury, Christchurch, New Zealand, 1975.
55. James, K.R. A Study of Branch Dynamics on an Open Grown Tree. *Arboric. Urban For.* **2014**, *40*, 125–134. Available online: <https://joa.isa-arbor.com/request.asp?JournalID=1&ArticleID=3318&Type=2> (accessed on 6 January 2022). [CrossRef]

56. Sellier, D.; Fourcaud, T. Crown Structure and Wood Properties: Influence on Tree Sway and Response to High Winds. *Am. J. Bot.* **2009**, *26*, 885–896. Available online: <https://www.jstor.org/stable/27733419> (accessed on 6 January 2022). [CrossRef]
57. Telewski, F. *Wind-Induced Physiological and Developmental Responses in Trees*; Published in Coutts MP; Wind and Trees; Grace, J., Ed.; Cambridge University Press: Cambridge, UK, 1995.
58. Nicoll, B.C.; Gardiner, B.A.R.B.; Peace, A.J. Anchorage of Coniferous Trees in Relation to Species, Soil Type, and Rooting Depth. *Can. J. For. Res.* **2006**, *36*, 1871–1883. Available online: <https://cdnsiencepub.com/doi/10.1139/x06-072> (accessed on 6 January 2022). [CrossRef]
59. Nicoll, B.; Gardiner, B.; Peace, A. Improvements in anchorage provided by the acclimation of forest trees to wind stress. *Forestry* **2008**, *81*, 389–398. [CrossRef]
60. Telewski, F. Is windswept tree growth negative thigmotropism? *Plant Sci.* **2012**, *184*, 20–28. [CrossRef]
61. Badel, E.; Ewers, F.; Cochard, H.; Telewski, F. Acclimation of mechanical and hydraulic functions in trees: Impact of the thigmomorphogenetic process. *Front. Plant Sci.* **2015**, *6*, 266. [CrossRef]
62. Shigo, A. *A New Tree Biology Dictionary*; Shigo and Trees Associates: Snohomish, WA, USA, 1986.
63. Blankenhorn, P. *Wood: Sawn Materials. Encyclopedia of Materials: Science and Technology*; Elsevier Ltd.: Pergamon, Turkey, 2001.
64. McDonald, A.; Donaldson, L. *Constituents of wood. Encyclopedia of Materials: Science and Technology*; Elsevier Ltd.: Pergamon, Turkey, 2001.
65. Yamamoto, H.; Ruelle, J.; Arakawa, Y.; Yoshida, M.; Clair, B.; Gril, J. Origin of the characteristic hygro-mechanical properties of the gelatinous layer in tension wood from Kunugi oak (*Quercus acutissima*). *Wood Sci. Technol.* **2010**, *44*, 149–163. [CrossRef]
66. Fratzl, P.; Weinkamer, R. Nature's hierarchical materials. *Prog. Mater. Sci.* **2007**, *52*, 1263–1334. [CrossRef]
67. Gibson, L.J. Biomechanics of cellular solids. *J. Biomech.* **2005**, *38*, 377–399. [CrossRef] [PubMed]
68. Fengel, D.; Wegener, G. *Wood: Chemistry, Ultrastructure, Reactions*; De Gruyter: Berlin, Germany, 1989.
69. Keckes, J.; Burgert, I.; Fruhmann, K.; Muller, M.; Kolln, K.; Hamilton, M.; Burghammer, M.; Roth, S.V.; Stanzl-Tschegg, S.; Fratzl, P. Cell-wall recovery after irreversible deformation of wood. *Nat. Mater.* **2003**, *2*, 810–814. [CrossRef] [PubMed]
70. Koehler, L.; Spatz, H. Micromechanics of Plant Tissues beyond the Linear-Elastic Range. *Planta* **2002**, *215*, 33–40. Available online: <https://link.springer.com/content/pdf/10.1007/s00425-001-0718-9.pdf> (accessed on 6 January 2022). [CrossRef] [PubMed]
71. Fratzl, P.; Burgert, I.; Gupta, H. On the role of interface polymers for the mechanics of natural polymeric composites. *Phys. Chem. Chem. Phys.* **2004**, *6*, 5575–5579. [CrossRef]
72. Dargahi, M.; Newson, T.; Moore, J.R. A Numerical Approach to Estimate Natural Frequency of Trees with Variable Properties. *Forests* **2020**, *11*, 915–935. [CrossRef]
73. Coutts, M.P. Components of tree stability in Sitka spruce on peaty gley soil. *Forestry* **1986**, *59*, 173–197. [CrossRef]
74. Giurgiu, V.; Decei, I. *Biometria Arborilor din România*; Editura Snagov: București, Romania, 1997.
75. Lundström, T.; Jonsson, M.J.; Kalberer, M. The root–soil system of Norway spruce subjected to turning moment: Resistance as a function of rotation. *Plant Soil* **2007**, *300*, 35–49. [CrossRef]
76. Mayer, H. Wind induced tree sways. *Trees* **1987**, *1*, 195–206. [CrossRef]
77. Hale, S.; Gardiner, B.; Wellpott, A.; Nicoll, B.; Achim, A. Wind loading of trees: Influence of tree size and competition. *Eur. J. For. Res.* **2010**, *131*, 203–217. [CrossRef]
78. Duryea, M.; Kampf, E.; Littell, R.; Rodriguez-Pedraza, C. Hurricanes and the Urban Forest II: Effects on Tropical. *Arboric. Urban For.* **2007**, *33*, 98–112. Available online: <https://hort.ifas.ufl.edu/treesandhurricanes/documents/pdf/EffectsOnTropicalAndSubtropicalTreeSpecies.pdf> (accessed on 6 January 2022). [CrossRef]
79. Kane, B. Tree failure following a wind storm in Brewster, Massachusetts, USA. *Urban For. Urban Green.* **2008**, *7*, 15–23. [CrossRef]
80. Peltola, H.; Kellomäki, S.; Väisänen, H.; Ikonen, V.-P. A Mechanistic Model for Assessing the Risk of Wind and Snow Damage to Single Trees and Stands of Scots Pine, Norway Spruce, and Birch. *Can. J. For. Res.* **1999**, *29*, 647–661. Available online: <https://cdnsiencepub.com/doi/10.1139/x99-029> (accessed on 6 January 2022). [CrossRef]
81. Kellomäki, S.; Peltola, H. *Silvicultural Strategies for Predicting Damage to Forests from Wind, Fire and Snow: Integrating Tree, Site and Stand Properties with Geographical Information Systems and Regional Environmental Models to Evaluate Options for Forest Management*; European Community: Brussels, Belgium, 1998.
82. Morgan, J.; Cannell, M.G.R. Shape of tree stems: A re-examination of the uniform stress hypothesis. *Tree Physiol.* **1994**, *14*, 49–62. [CrossRef]
83. Sunley, J.-G. Grade Stresses for Structural Timbers. *For. Prod. Res. (Bull.)* **1968**, *47*, 1–18. Available online: <https://catalogue.nla.gov.au/catalog/940485> (accessed on 6 January 2022).
84. Petty, J.A.; Worrell, R. Stability of coniferous tree stems in relation to damage by snow. *Forestry* **1981**, *54*, 115–128. [CrossRef]
85. Jones, H.G. *Plants and Microclimate. A Quantitative Approach to Environmental Plant Physiology*; Cambridge University Press: Cambridge, UK, 1983. [CrossRef]
86. Peltola, H.; Kellomäki, S. A mechanistic model for calculating windthrow and stem breakage of Scots pines at stand edge. *Silva Fenn.* **1993**, *27*, 99–111. [CrossRef]
87. Neild, S.A.; Wood, C.J. Estimating stem and root-anchorage flexibility in trees. *Tree Physiol.* **1999**, *19*, 141–151. [CrossRef] [PubMed]

88. Popa, A.; Ilieș, N.M. *Fundații*; Casa Cărții de Știință: Cluj-Napoca, Romania, 2013; pp. 87–88.
89. Jonsson, M.J.M.J.; Foetzki, A.; Kalberer, M.; Lundström, T.; Ammann, W.; Stöckli, V. Root-soil rotation stiffness of Norway spruce (*Picea abies* (L.) Karst) growing on subalpine forested slopes. *Plant Soil* **2006**, *285*, 267–277. [[CrossRef](#)]
90. Vogel, S.; Davis, K.K. *Cat's Paws and Capulps: Mechanical Worlds of Nature and People*; W. W. Norton & Company: New York, NY, USA, 2000.
91. Cattano, C.; Nikou, T.; Klotz, L. Teaching systems: Thinking and biomimicry to civil engineering students. *J. Prof. Issues Eng. Educ. Pract.* **2011**, *137*, 176–182. [[CrossRef](#)]
92. Knippers, J.; Speck, T. Design and Construction Principles in Nature and Architecture. *Bioinspir. Biomim.* **2012**, *7*, 015002. Available online: <https://iopscience.iop.org/article/10.1088/1748-3182/7/1/015002/meta> (accessed on 6 January 2022). [[CrossRef](#)] [[PubMed](#)]
93. Benyus, J. *Biomimicry*; William Morrow and Company: New York, NY, USA, 1997.
94. Xing, D.; Chen, W. Systematic method of applying structural characteristics of natural organisms to mechanical structures. *Trans. Tianjin Univ.* **2011**, *17*, 303–307. [[CrossRef](#)]
95. Aviation Weather Center (AWC). *Wood Frame Construction Manual Workbook: Design of Wood Frame Buildings for High Wind, Snow and Seismic Loadings*; AWC: Virginia, NV, USA, 2005.
96. Ennos, R. *Trees: Magnificent Structures*; The Natural History Museum: London, UK, 2001.
97. Grudnicki, F. Biomecanica Sistemelor Radicelare ale Arborilor Forestieri (“Biomechanics of Root Systems of Forest Trees”). *Rev.-Bucov. For.* **2003**, *11*, 39–48. Available online: [http://bucovina-forestiera.ro/BF%20old%20site/Bucovina%20forestiera/www.bucovina-forestiera.ro/arhiva/2003/11\(1\)/biomecanica-sistemelor-radicelare-ale-arborilor-forestieri.pdf](http://bucovina-forestiera.ro/BF%20old%20site/Bucovina%20forestiera/www.bucovina-forestiera.ro/arhiva/2003/11(1)/biomecanica-sistemelor-radicelare-ale-arborilor-forestieri.pdf) (accessed on 6 January 2022).
98. Schmier, S.; Bold, G.; Buck, G.; Klang, K.; Lauer, C.; Toader, N.; Gericke, O.; Haase, W.; Schäfer, I.; Schmauder, S.; et al. Hohe Belastungen sicher überstehen. In *Bionisch Bauen*; Birkhäuser: Berlin, Germany; Boston, MA, USA, 2019; pp. 54–73. [[CrossRef](#)]
99. Ostertag, A.; Toader, T.-N.; Bertsche, B.; Sobek, W. System-Safety in the Application of Adaptive Load-Bearing Structures. In Proceedings of the Annual Reliability and Maintainability Symposium, Orlando, FL, USA, 28–31 January 2019; IEEE Proceedings. Available online: <https://ieeexplore.ieee.org/document/8769000> (accessed on 6 January 2022).
100. Chirișescu, M. Utilizarea Precomprimării la Elemente Prefabricate Lungi din Beton, Solicitate Preponderent la Compresiune cu Încovoiere. Ph.D. Thesis, UTCN, Cluj-Napoca, Romania, 2016.
101. Chirișescu, M.; Kiss, Z.; Mureșan, R.-M. A finite element numerical simulation on different types of prestressed concrete columns. In Proceedings of the 13th International Scientific Conference VSU 2013, Sofia, Bulgaria, 22–24 June 2013.
102. Chirișescu, M.; Kiss, Z.; Mureșan, R.-M. An experimental study on a series of three types of prestressed concrete columns. In Proceedings of the 13th International Scientific Conference VS 2013, Sofia, Bulgaria, 22–24 June 2013.
103. Kovacs, B. Un Algoritm de Calcul Pentru Stâlpi din Beton Precomprimat. Master’s Thesis, UTCN, Cluj-Napoca, Romania, 2022.
104. Kovacs, B.; Toader, T.-N. An automated Algorithm for the Sectional Analysis of Reinforced and Prestressed Concrete Columns. *J. Appl. Eng. Sci.* **2022**, *12*, 61–70. Available online: <https://sciendo.com/fr/article/10.2478/jaes-2022-0010> (accessed on 6 January 2022). [[CrossRef](#)]
105. Rozian, D. Influența Ligninei Asupra Rezistenței la Compresiune a Betonului și Asupra Aderenței Armăturii în Beton. Master’s Thesis, UTCN, Cluj-Napoca, Romania, 2022.
106. Jahanban-Esfahlan, A.; Ostadrahimi, A.; Tabibiazar, M.; Amarowicz, R. A comprehensive review on the chemical constituents and functional uses of walnut (*Juglans* spp.) husk. *Int. J. Mol. Sci.* **2019**, *20*, 3920. [[CrossRef](#)] [[PubMed](#)]
107. Sareena, C.; Sreejith, M.; Ramesan, M.; Purushothaman, E. Biodegradation behaviour of natural rubber composites reinforced with natural resource fillers—Monitoring by soil burial test. *J. Reinf. Plast. Compos.* **2014**, *33*, 412–442. [[CrossRef](#)]
108. Kiss, Z.; Balint, K.; Toader, N.; Nagy, Z. A long span structure in Romania. In Proceedings of the IABSE Symposium: Long Span Bridges and Roofs—Development, Design and Implementation, Kolkata, India, 24–27 September 2013. [[CrossRef](#)]
109. Toader, T.-N.; Schmeer, D.; Sobek, W. Concept for an Onshore Tower Structure Made of UHPFRC Segments for Wind Turbines. *Acta Tech. Napoc. Civ. Eng. Archit.* **2019**, *62*, 5–25. Available online: [https://oldconstructii.utcluj.ro/ActaCivilEng/download/atn/ATN2019\(1\)_1.pdf](https://oldconstructii.utcluj.ro/ActaCivilEng/download/atn/ATN2019(1)_1.pdf) (accessed on 6 January 2022).
110. Toader, N.; Kiss, Z. Experimental Tests on a Precast Concrete Frame Structure Subjected to Lateral Loads. *Bul. Institutului Politeh. Din Iasi—Secția Construcții. Arhit.* **2014**, *54*, 110–119. Available online: <http://www.bipcons.ce.tuiasi.ro/Archive/475.pdf> (accessed on 6 January 2022).
111. Maier, M.; Siegel, D.; Thoben, K.D.; Niebuhr, N.; Hamm, C. Transfer of natural micro structures to bionic lightweight design proposals. *J. Bionic Eng.* **2013**, *11*, 469–478. [[CrossRef](#)]
112. American Institute of Steel Construction (AISC). *Seismic Provisions for Structural Steel Buildings*; AISC: Chicago, IL, USA, 2005.
113. National Research Council Canada. *National Building Code of Canada*; National Research Council Canada: Ottawa, ON, Canada, 1995.
114. Grigorian, M.; Grigorian, C. Performance Control: New Elastic-Plastic Design Procedure for Earthquake Resisting Moment Frames. *J. Struct. Eng.* **2012**, *138*, 812–821. Available online: [https://ascelibrary.org/doi/abs/10.1061/\(ASCE\)ST.1943-541X.0000515](https://ascelibrary.org/doi/abs/10.1061/(ASCE)ST.1943-541X.0000515) (accessed on 6 January 2022). [[CrossRef](#)]

115. CEN European Commission for Standardization. *Eurocode 8: Design of Structures for Earthquake Resistance. Part 1: General Rules, Seismic Actions and Rules for Buildings*; CENELEC: Bruxelles, Belgium, 2006.
116. MDRAP. P100-1/2013. *Cod de Proiectare Seismică—Partea I—Prevederi Pentru Clădiri*; Monitorul Oficial al României: București, Romania, 2019.

Disclaimer/Publisher's Note: The statements, opinions and data contained in all publications are solely those of the individual author(s) and contributor(s) and not of MDPI and/or the editor(s). MDPI and/or the editor(s) disclaim responsibility for any injury to people or property resulting from any ideas, methods, instructions or products referred to in the content.